Accepted Manuscript

The proteome map of the escamolera ant (Liometopum apiculatum Mayr) larvae reveals immunogenic proteins and several hexamerin proteoforms

José A. Huerta-Ocampo, María S. García-Muñoz, Aida J. Velarde-Salcedo, Eric E. Hernández-Domínguez, Jorge L. González-Escobar, Alberto Barrera-Pacheco, Alicia Grajales-Lagunes, Ana P. Barba de la Rosa
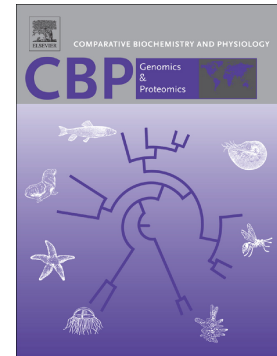
Please cite this article as: José A. Huerta-Ocampo, María S. García-Muñoz, Aida J. Velarde-Salcedo, Eric E. Hernández-Domínguez, Jorge L. González-Escobar, Alberto Barrera-Pacheco, Alicia Grajales-Lagunes, Ana P. Barba de la Rosa , The proteome map of the escamolera ant (Liometopum apiculatum Mayr) larvae reveals immunogenic proteins and several hexamerin proteoforms. Cbd (2018), doi:10.1016/j.cbd.2018.07.004

The proteome map of the *escamolera* ant (*Liometopum apiculatum* Mayr) larvae reveals immunogenic proteins and several hexamerin proteoforms

José A. Huerta-Ocampo[a,b], María S. García-Muñoz[c], Aida J. Velarde-Salcedo[a], Eric E. Hernández-Domínguez[a,‡], Jorge L. González-Escobar[a], Alberto Barrera-Pacheco[a], Alicia Grajales-Lagunes[c,*], Ana P. Barba de la Rosa[a,*]

[a]*IPICyT, Instituto Potosino de Investigación Científica y Tecnológica A.C., Camino a la Presa San José No. 2055, Lomas 4a Sección 78216, San Luis Potosí, S.L.P., México.*

[b]*CONACYT-Centro de Investigación en Alimentación y Desarrollo A.C. Carretera a La Victoria Km 0.6, Edificio C. C.P 83304 Hermosillo, Sonora.*

[c]*Facultad de Ciencias Químicas, Universidad Autónoma de San Luis Potosí, Av. Dr. Nava No.6, Zona Universitaria, C.P. 78200, San Luis Potosí, S.L.P., México.*

[‡]*Current address: CONACYT-Instituto de Ecología A.C. (INECOL) Carretera antigua a Coatepec 351, El Haya, Xalapa c.p. 91070, Veracruz, México.*

Running title*: Liometopum apiculatum proteomics and hexamerin characterization*

ms has 37 pages, 1 table, 7 Figures, 1 Supplementary Excel file, 3 Supplementary Info,

*Corresponding authors:

A.P. Barba de la Rosa (E-mail: apbarba@ipicyt.edu.mx); A. Grajales-Lagunes (E-mail: grajales@uaslp.mx).

1

Abstract

The larvae of *escamolera* ant (*Liometopum apiculatum* Mayr*)* have been considered a delicacy since Pre-Hispanic times. The increased demand for this stew has led to massive collection of ant nests. Yet biological aspects of *L. apiculatum* larvae remain unknown, and mapping the proteome of this species is important for understanding its biological characteristics. Two-dimensional gel electrophoresis (2-DE) followed by liquid chromatography-tandem mass spectrometry (LC-MS/MS) analysis was used to characterize the larvae proteome profile. From 380 protein spots analyzed, 174 were identified by LC-MS/MS and homology search against the Hymenoptera subset of the NCBInr protein database using the Mascot search engine. Peptide *de novo* sequencing and homology-based alignment allowed the identification of 36 additional protein spots. Identified proteins were classified by cellular location, molecular function, and biological process according to the Gene Ontology annotation. Immunity- and defense-related proteins were identified including PPIases, FK506, PEBP, and chitinases. Several hexamerin proteoforms were identified and the cDNA of the most abundant protein detected in the 2-DE map was isolated and characterized. *L. apiculatum* hexamerin (*LaHEX,* GeneBank accession no. MH256667) contains an open reading frame of 2199 bp encoding a polypeptide of 733 amino acid residues with a calculated molecular mass of 82.41 kDa. LaHEX protein is more similar to HEX110 than HEX70 from *Apis mellifera.* Down-regulation of *LaHEX* was observed throughout ant development. This work represents the first proteome map as well as the first hexamerin characterized from *L. apiculatum* larvae.

1. Introduction

Insects are an excellent alternative protein source to meet the increased food demand of the rapidly growing global population (FAO, 2013). Entomophagy is practiced primarily in regions of Asia, Africa, and Latin America, where insects are considered as delicacy. Recently, entomophagy has been promoted in Western societies, and its practice has been successfully introduced in The Netherlands (Jansson and Berggren, 2015). Worldwide, there are an estimated 10 millions of insects/km^2, of which approximately 2,000 species are edible (Van Huis et al., 2013). The most common insects used as food are beetles belonging to the Coleoptera order (31%), caterpillars from Lepidoptera order (18%), and bees, wasps, and ants of the Hymenoptera order (14%) (Ramos-Elorduy et al., 2008; Van Huis et al., 2013).

In Mexico, there are 525 documented ants species (CONABIO, 2008), 5 of which are considered edible: the leafcutter ants (*Atta cephalotes* L. and *Atta Mexicana Bourmeir*), the escamolera ant (*Liometopum apiculatum* Mayr), and the honeypot ants (*Myrmecosistus melliger* Llave (Luc.) and *Myrmecosistus mexicanus* W.) (Ramos-Elorduy and Levieux, 1992; Ramos-Elorduy and Pino, 2003). *L. apiculatum* belongs to the Hymenoptera order, Formicidae family, and Dolichoderinae subfamily (Ward et al., 2010). *L apiculatum* was originally named *Formica masonium*, but based on workers ants collected in Mexico, Mayr (1870) renamed them as *L. apiculatum* (Lara-Juárez et al., 2015). *L. apiculatum* larvae are known in Mexico as "escamoles", derived from the

Nahuatl (language of the Aztecs) "azcatlmolli" from *azcatl*=ant and *molli*=stew. Escamoles have been consumed since pre-Hispanic times, and currently are considered a delicacy (Ramos-Elorduy and Pino, 2003). *L. apiculatum* larvae are rich in proteins (37.3 to 39.7%), which contain most of the essential amino acids such as lysine, leucine, methionine, tyrosine, and tryptophan. The larvae also contain fats (36.87%), and carbohydrates (19.2%) as well as vitamins including A, C, B1, B2, B3 (Ladrón De Guevara et al., 1995; Ramos-Elorduy et al., 2002; Del Toro et al., 2009; Ramos-Rostro et al., 2012; Melo-Ruiz et al., 2013). Despite this current information about the nutritional composition of *L. apiculatum* larvae, information regarding their molecular protein composition remains unknown.

Genome and transcriptome data generated via global gene expression analysis for several organisms are insufficient to fulfill the necessary understanding in terms of physiology and biological processes controlled by proteins. Proteins represent the most fundamental and biologically active agents controlling every cellular process (Pomastowski and Buszewski, 2014). Proteomics analysis is the most promising tool to understand the molecular mechanisms that dictate the biological events of an organism, not only by means of protein quantity or cellular location, but also the accumulation of various protein species as well as their posttranslational modifications (Kaji et al., 2000).

Considering the limited knowledge about biomolecules present in *L. apiculatum* larvae and their economic importance as an alternative dietary protein source, the aim of this work was to generate information about the proteins present in larvae of *L. apiculatum* Mayr that could help to better understanding of their nutritional and physiology properties. Our results demonstrate that protein composition in *L. apiculatum*

larvae is associated with different metabolic pathways (carbohydrates, amino acids, and lipids). Results also have shown the presence of immunogenic and defense proteins. Several hexamerin proteoforms were identified, and the full open reading frame of the most abundant was isolated by means of Rapid Amplification of cDNA Ends (RACE). *L. apiculatum* hexamerin (LaHEX) was characterized *in silico* and its expression was examined at different stages of ant development.

2. Materials and methods

2.1. Sample collection

Liometopum apiculatum Mayr larvae samples were collected at Pocitos municipality of Charcas, San Luis Potosi, Mexico. Biological triplicates were collected from three different colonies. Each replicate contained a minimum of 50 larvae of 18-25 days of age. Samples were transported on ice to the lab and contaminant soil was removed with a soft wash of distilled sterile water. Larvae were ground with liquid nitrogen in a coffee grinder (Braun, Naucalpan, Mexico) to obtain a fine powder. Powders of each biological triplicate were divided into two samples and stored at -80°C until use. One sample was used for total protein extraction, and the second sample for RNA extraction.

2.2. Total soluble protein extraction

Larvae powder samples (5 g) were suspended in cold acetone, mixed by vortexing for 2 min and centrifuged for 10 min at 13,000 x g at 4°C (Super T21; Sorvall, Kendro Laboratory Products, Newton, CT, USA). Supernatants were discarded, and the pellets were dried under vacuum (Vacufuge Plus, Eppendorf, Hamburg, GER). Dried pellets

were suspended in rehydration buffer (8 M urea, 2% CHAPS, 0.56% dithiothreitol (DTT), and 0.002% bromophenol blue), and sonicated at 20 kHz (GE-505, Ultrasonic Processor, Sonics & Materials Inc., Newtown, CT, USA) for 3 min. After sonication, samples were centrifuged for 10 min at 13,000 x *g* at 4°C (Super T21; Sorvall). Supernatants were filtered through Miracloth filters (Merck KGaA, Darmstadt, GER) and centrifuged for 10 min at 13,000 x g at 4°C. The resulting supernatants were precipitated with 10 parts of 0.1 M ammonium acetate and incubated overnight at -20 °C. After 30 min of centrifugation at 13,000 x g at 4°C, the protein pellets were washed once in cold methanol and three times in cold acetone, dried, and finally suspended in rehydration buffer. Protein concentration was determined using the Protein Assay reagent (Bio-Rad, Hercules, CA, USA) with bovine serum albumin (BSA) as the standard.

2.3. Two-dimensional electrophoresis (2-DE)

Isoelectric focusing (IEF) was carried out onto 24 cm IPG linear gradient strips pH 3-10 and 5-8 (Bio-Rad). Strips were rehydrated with 2.25 mg of total protein. Focusing was conducted at 20°C with an Ettan IPGphor system (GE Healthcare, Piscataway, NJ, USA) at constant 50 mA per strip under the following conditions: (I) 150 V gradient for 2 h, (II) 300 V gradient for 2 h, (III) 1000 V gradient for 2 h, (IV) 3000 V gradient for 3 h, (V) 6000 V gradient for 3 h, and (VI) holding at 6000 V for 10 h. After IEF, the IPG strips were equilibrated for 15 min in equilibration buffer (6 M urea, 30% glycerol, 2% SDS, 50 mM Tris-HCl buffer pH 8.8) containing 1% DTT. Strips were placed directly onto 13% polyacrylamide-SDS slab gels, and separation was conducted using the EttanDaltsix

Electrophoresis unit (GE Healthcare). Gels were stained with PhastGel Blue R (GE Healthcare), and documented with Pharos FX Plus Molecular Imager (Bio-Rad). Image analysis was performed with PDQuest 2-D Analysis Software v8.0 (Bio-Rad). Experimental molecular mass of each protein spot was estimated by comparison with molecular weight standards (BenchMark Protein Ladder, Invitrogen, Carlsbad, CA, USA). Experimental *pI* was estimated by migration of protein spots on the IPG linear gradient strips. Three different extractions were prepared for each biological replicate and for each pH range (3-10 and 5-8).

2.4. In-gel digestion and tandem mass spectrometry analysis (LC-MS/MS)

Protein spots were excised from the 2-DE gels, distained, and reduced with 10 mM DTT in 25 mM ammonium bicarbonate followed by protein alkylation with 55 mM iodoacetamide. Proteins were digested overnight with sequencing grade trypsin (Promega, Madison, WI, USA) at 37°C. Separation and analysis of tryptic peptides was performed with a nano ACQUITY UPLC System (Waters, Milford, MA, USA) coupled to a SYNAPT HDMS Q-TOF (Waters) as previously reported (Huerta-Ocampo et al., 2014).

2.5. Database search and protein identification

The MS/MS spectra datasets were searched against the *Hymenoptera* subset of the NCBInr protein database (219 251 sequences; 79 008151 residues, September 2013) using the MASCOT search engine v.2.3 (Matrix Science, London, UK available at http://www.matrixscience.com). Trypsin was used as the specific protease, and one

missed cleavage was allowed. The mass tolerance for precursor and fragment ions was set to 20 ppm and 0.1 Da, respectively. Carbamidomethyl cysteine was set as fixed modification and oxidation of methionine was specified as variable modification. Identifications were considered successful when significant MASCOT scores (≥30) were obtained, indicating the identity or extensive homology at $p<0.05$.

2.6. De-novo sequencing and FASTA peptide homology

LC-MS/MS data from protein spots not identified by database search with MASCOT search engine was used to perform peptide *de novo* sequencing using Protein Lynx Global SERVER™ V 2.4 (PLGS, Waters). Mass tolerance for precursor and fragment ions was set to 20 ppm and 0.1 Da, respectively, whereas carbamidomethyl cysteine and oxidation of methionine were set as fixed and variable modification, respectively. FASTA algorithm (Pearson, 2000), available at https://www.ebi.ac.uk/Tools/sss/fasta/ and http://fasta.bioch.virginia.edu/fasta_www2/fasta_www.cgi?rm=select&pgm=fap, was used to identify highly similar regions between the de novo predicted peptides and proteins from UniProt Knowledgebase. Peptide alignments with more than 80% of identity were considered as significant (Mackey et al., 2002).

2.7. *Gene Ontology analysis*

Identified proteins were grouped into different functional categories according to data from Gene Ontology (http://www.geneontology.org/). Proteins with multiple likely isoforms were considered as one protein. Unique proteins were submitted to a Gene Ontology (GO) analysis using Blast2GO v3.0.8 (www.blast2go.org) (Conesa et al.,

2005). Protein sequences were compared against the NCBInr protein database (BLAST-P) of the most likely *L. apiculatum* orthologous (previously obtained after MS/MS data-based protein identification). The input parameters used were as follows: number of BLAST hits requested for each query, 20; BLAST expect value (i.e., eValue), 1^{e-25}. Then, GO mapping was performed to obtain GOs for hits retrieved by the BLAST-P step and annotation was obtained. Annotation parameters were as follow: e-value hit filter; 1^{e-25}; annotation cutoff, 55; and GO weight 5, graphs of biological processes, molecular functions and cellular components of the proteins with GO annotations were obtained with the Make Combined Graph Tool.

2.8. Hexamerin cDNA isolation and characterization

Primers for hexamerin amplification were designed using the peptide information obtained from LC-MS/MS data, bioinformatics analysis, and multiple sequence alignments (Clustal Omega at http://www.ebi.ac.uk/Tools/msa/clustalo/) with annotated and predicted Hymenoptera hexamerin cDNA sequences deposited in NCBI database. Oligonucleotides within conserved regions were designed with MacVector Software (MacVector Inc., Apex, NC, USA). RNA was extracted from *L. apiculatum* larvae of three independent collections with Trizol Reagent (Thermo Fischer Scientific Inc., Waltham, MA, USA) following the manufacturer's instructions. RACE was performed with the SMARTer RACE5'/3' kit (Clontech Laboratories Inc., Mountain View, CA, USA) and Phusion High Fidelity DNA polymerase (Thermo). Subsequent gene specific oligonucleotides were designed and verified with MacVector Software. The list of oligonucleotides used is shown in **Supplementary Table S1**. All oligonucleotides were

synthesized by Sigma-Aldrich (St. Louis, MO, USA). Amplified fragments were analyzed on a 1.2% agarose gels, cDNA bands were excised from gel, and purified with StrataPrep PCR Purification Kit (Agilent Technologies, Santa Clara, CA, USA). Fragments were sequenced by Laboratorio Nacional de Biotecnología Agrícola, Médica y Ambiental (IPICYT, Mexico) in a 3130 Genetic Analyzer (Applied Biosystems, Foster City, CA, USA). Nucleotide sequences were checked by chromatogram quality and assembled with a minimum match of 75%. *Liometopum apiculatum* (LaHEX) protein sequence was predicted by *in silico* translation using the ExPASy server (http://www.expasy.org). Conserved hemocyanin N, M, and C domains were identified using the CD database (https://www.ncbi.nlm.nih.gov/Structure/cdd/cdd.shtml) and HMMER web server (ebi.ac.uk; Finn et al., 2015). Phosphorylation sites were predicted with NetPhos (expasy.org). Sequence similarities of LaHEX with 23 hexamerins, hemocyanins and arylphorins deposited at GenBank were determined using the Clustal omega (http://www.ebi.ac.uk/Tools/msa/clustalo/).

Phylogenetic analysis was performed using Molecular Evolutionary Genetics Analysis 6 (MEGA 6, https://www.megasoftware.net/). Multiple alignments of amino acid sequences were performed using Muscle software (https://www.ebi.ac.uk/Tools/msa/muscle/). The phylogenetic tree was constructed using the Maximum-likelihood method with a Jones–Thornton–Taylor (JTT) model to estimate the distances. The statistical analysis was performed with at least 1000 bootstrap repetitions. The circular phylogenetic tree was completed using the online Interactive Tree of Life resource (Letunic and Bork, 2007).

2.9. Hexamerin regulation through ant development

Frozen powder of *L. apiculatum* larvae (50 mg) of each biological replicate was used for total RNA extraction using TRIzol Reagent (Invitrogen) following the manufacturer´s instructions. RNA was quantified using the NanoDrop 1000 (Thermo), and its integrity was evaluated by electrophoresis in formaldehyde RNA gel. To remove genomic DNA, 1 µg total RNA was incubated for 15 min at room temperature in presence of 1 µL of deoxyribonuclease I amplification grade at 1 U/µL (Invitrogen), according to manufacturer´s instructions. Primers for hexamerin and hemocyanin expression analysis as well the ribosomal protein L18 *(RPL18)* gene, which was set as reference gene (**Supplementary Table S2**), were designed using the Primer3 program (Rozen et al., 2000). Quantitative real time-polymerase chain reaction (qRT-PCR) analysis was performed using a RT-PCR System (Bio-Rad) in a 10 µL-reaction volume containing 0.5 µL of cDNA template, 5 µL Fast Eva Green Supermix (Bio-Rad), 0.5 µL of each primer (10 mM), and 3.5 µL of nuclease-free water. Relative expression levels for validated genes were calculated by the $\Delta\Delta C_T$ method as described by Livak and Schmittgen (2001). All samples were run in triplicates.

3. Results

3.1. 2-DE proteome profile of L. apiculatum larvae

L. apiculatum larvae proteome profile was analyzed using 2-DE. Protein separation on the first dimension was performed on IPG strips with a pH range of 3-10. As shown in **Supplementary Figure S1A**, most of the proteins were located between pH 5-8. Therefore, IPG strip with a pH in this range was used, which resulted in higher

resolution (**Supplementary Figure S1B**). To avoid losing information at pH extremes, a composed 2-DE map of *L. apiculatum* larvae was generated, and a total of 380 proteins spots were analyzed (**Figure 1)**. Although *L. apiculatum* genome is not sequenced and only few proteins (28) and nucleotide sequences (38) for this organism are reported in public databases, homology database search against organisms belonging to the order Hymenoptera allowed the identification of 174 protein spots (46%). In 23 cases, more than one protein per spot was identified (**Table 1, Supplementary File S1**). The number and score of peptides matched to proteins were generally better from organisms belonging to the Formicidae family than from other members of the Hymenoptera order. In some cases, the best matches were against non-ant Hymenoptera (**Table 1**). Interestingly, in most of homology database identifications carried out with the Mascot search engine, different peptides belonging to the same putative identified protein but matched against different organisms were observed (some examples are shown in **Supplementary File S2**).

3.2. Peptide de novo sequencing of unidentified protein spots

MS/MS data sets of protein spots that were not identified by homology database search with the Mascot search engine were subjected to peptide de novo sequencing and FASTA homology search against the Uniprot Knowledgebase (Vyatkina, 2017). Most of the significant alignments were against non-ant Hymenoptera, whereas 14 were for ants and only two for other insects. Based on this approach, 36 additional protein spots were identified. An example, for the identified Cu-Zn superoxide dismutase, is presented in **Figure 2**. Most of the identified peptides corresponded to hexamerins and

hemocyanins (**Supplementary File S3, Supplementary Figure S2**), showing the high diversity of proteoforms of these two proteins in the *L. apiculatum* larvae proteome.

3.3. Functional annotation of L. apiculatum larvae identified proteins

Proteins identified by LC-MS/MS were assigned into functional groups according to the GO annotation using Blast2GO (Conesa et al., 2005). From 146 unique identified proteins, 134 were classified using the available annotations (**Figure 3**). In the molecular function ontology, the main groups were catalytic activity, binding, structural molecules, and transport. In relation to their cellular component; proteins were grouped to organelle, cell, macromolecular complex, and membrane proteins. According to the biological process, the main categories were related to metabolic and cellular processes, biological regulation, biogenesis, and single-organism process.

3.4. Hexamerins and hemocyanins proteforms in L. apiculatum proteome map

Multiple hexamerins proteoforms (spots 70, 342, 354, 355, 357, and 359) were detected by proteomics (**Table 1**), and several others were identified by *de novo* sequencing approach (**Supplementary Table S3 and Supplementary Figure S2**). Hemocyanin was identified in *L. apiculatum* larvae proteome map in only one spot (351), but using *de novo* sequencing, 11 more proteoforms were identified. Hemocyanin is present in many insects (Amore et al., 2011), but its presence or absence in distinct group of insects is unknown (Burmester and Hankeln, 2007).

Because the high amount of hexamerin proteoforms detected in the *L. apiculatum* larvae proteomic map, coupled with absence of information about *L. apiculatum*

13

hexamerins, as well as the interest in hexamerins´s evolutionary relationships (Burmester, 1999 and 2015), we proceeded with the cDNA isolation of the most abundant *L. apiculatum* larvae hexamerin (spot 70).

3.5. L. apiculatum hexamerin (LaHEX) isolation and characterization

LaHEX cDNA was cloned (GenBank accession no. MH256667) and found to contain a 2199 bp open reading frame of encoding a 733 amino acid residues with a predicted molecular mass of 82.41 kDa and an isoelectric point of 5.66 (**Supplementary Figure S3**). The evolutionary relationship of LaHEX was analyzed by comparison with different hexamerins and hemocyanins sequences deposited at GenBank from different Orders including Hymenoptera, Blatodea, Decapoda, Lepidoptera, Coleoptera, and Diptera. The Phylogenetic tree, shown in **Figure 5**, reflects the molecular grouping of different insect orders. Within the Hymenoptera order, LaHEX was grouped more closely with HEX110 than with the other *Apis mellifera* HEX**.** Clustal analysis shows regions corresponding to the conserved Hemocyanin (N, M, and C) domains presented in hexamerins (**Supplementary Figure S4)**. A schematic diagram of LaHEX structure compared with the most well-known hexamerins, the HEX100 and HEX70 from *Apis mellifera*, is presented in **Figure 6**. As observed, Hemocyanin C domain in LaHEX is larger than the domain reported for HEX110 (Martins et al., 2010).

4. Discussion

Proteomics is a powerful tool that has been used widely to analyze biochemical and physiological processes of insects including viral infection in *Bombyx mori* (Gao et al., 2017), resistance mechanisms in *Plutella xylostella* (Xia et al., 2016), testis development of *Bactrocera dorsalis* (Wei et al., 2018), as well as the innate immune response and reproductive proteins in *Drosophila melanogaster* (de Morais et al., 2005; Findlay and Swanson, 2010). Proteomics is a suitable tool for the discovery of unannotated genes/proteins using MS and bioinformatics approaches (Findlay et al., 2009).

Although newer shotgun-MS approaches have been developed, 2-DE MS remains a valuable top-down analytical approach (Oliveira et al., 2014). 2-DE proteomic maps allows for visualization of proteome in two dimensions, p*I* and MW, information that is lost when shotgun approaches are used (Magdeldin et al., 2014). 2-DE maps resolve thousands of intact protein species in a single run, enabling the identification of different protein isoforms and post-translational modifications (Oliveria et al., 2014; Pomastowski and Buszewski, 2014). For these reasons, 2-DE LC-MS/MS was used to obtain the *L. apiculatum* larvae proteome profile (Figure 1). Although the *L. apiculatum* genome is not yet sequenced, the 46% of resolved proteins spots were successfully identified by LC-MS/MS, and 36 more protein spots were identified using *de novo* sequencing and bioinformatics tools. Identified proteins were grouped according to its function such as metabolism, cell structure, transcription and translation, protein degradation, stress proteins, and other functions.

4.1. Proteins related with metabolism

4.1.1. Carbohydrate metabolism

In relation to the glycolysis pathway, several proteoforms of glyceraldehyde 3-phosphate dehydrogenase (spots 33, 36, 38, 39, 125), triose phosphate isomerase (spots 100, 101, 232, 233), were detected. Enolase (spots 140,146, 158, 199), an enzyme with functions both in and outside of the glycolytic pathway (Díaz-Ramos et al., 2012), was also detected. In insects, enolase is reported as one chorionic protein of the mature egg (Nguyen et al., 2013). Phosphoglycerate kinase (PGK, spots 140, 146, 147, 158, 199, and 348) was detected (**Table 1**) as well as the phosphoglycerate mutase (PGAM, spots 27 and 94). *Drosophila nubian* mutants disrupted in PGK showed reduced lifespan, abnormal motor behavior, and defective neurotransmitter release (Chiarelli et al., 2012). Spots 17, 42, and 77 were identified as nucleoside diphosphate kinase (NDPK). NDPK in insects helps to the successful development of the larval stage (Sinha et al., 2012).

4.1.2. Amino acids and purine metabolism

Among proteins related to amino acid metabolism, arginine kinase (AK, spot 226), an enzyme that catalyzes the reversible conversion of L-arginine to phosphoarginine (Bragg et al., 2012), was detected. Due to its important role in energy metabolism and because it is absent in vertebrates, AK is an excellent target for the development of new chemotherapeutic agents against parasitic diseases (Wu et al., 2008). Pterin-4α-carbinolamine dehydratase (PCD, spots 79, 81, and 360) is involved in the production of tetrahydrobiopterin (BH4). BH4 is an essential cofactor in phenylalanine metabolism

(Eskinazi et al., 1999), its deficiency in *Bombyx mori* larvae produces a colourless cuticle (Fujii et al., 2013).

Aminoacylase-1 (ACY-1, spots 222 and 223) hydrolyses N-acetyl amino acids into free amino acids as well the hydrolyzes fatty acid amino-acid conjugates (FACs) (Cheng et al., 2017). ACY1 may allow specialized larvae to obtain nitrogen supplies despite limitations in food heterogeneity (Kuhns et al., 2012; Cheng et al., 2017). Fumarylacetoacetate hydrolase (FAH, spot 110) catalyses the last enzymatic reaction in the tyrosine catabolism pathway. FAH silencing in insects did not affect survival, but FAH knockdown in adult females produced the complete suppression of reproduction (Sterkel and Oliveria, 2017). Spot 329 was identified as homocysteine S-methyltransferase. The regulation of homocysteine accumulation in young Drosophila leads to increased life span (Parkhitko et al., 2016). The bifunctional purine biosynthesis protein PurH (5-amino-4-imidazolecarboxamide ribonucleotide transformylase/IMP cyclohydrolase) was detected in spots 45 and 46. PurH catalyzes the last steps in the inosine 5-monophospahte synthesis pathway. This enzyme has been of particular interest for development of anticancer molecules (Bulock et al., 2002).

4.1.3. Lipid metabolism

The 3-hydroxyacyl-CoA dehydrogenase (spot 96) and the long-chain 3-ketoacyl-CoA thiolase (spot 127) are involved in fatty acid metabolism. In Drosophila, the deficiency of these proteins reduces lifespan and fecundity (Kishita et al., 2012). Spot 140 was identified as 4-hydroxybutyrate coenzyme A transferase, which plays a key role in butyrate formation in gut bacteria (Charrier et al., 2006; Zhang et al., 2009).

Medium-chain acyl-Co A dehydrogenase (MCAD, Spot 130) is involved in mitochondrial fatty acid β-oxidation, which fuels hepatic ketogenesis or fat-burn under conditions of low carbohydrate consumption. Short/branched chain acyl-CoA dehydrogenase (SBCAD, spots 344 and 349) is also involved in metabolism of fatty acids or short-branched chain amino acids; its deficiency leads to defects in L-isoleucine catabolism (Madsen et al., 2006).

4.2. Proteins related to cell structure

Both myophilin (spot 24) and stathmin (spot 177) were detected in *L. apiculatum* larvae. The first is a protein implicated in the regulation of smooth-muscle contractions and cytoskeletal organization (Horowitz et al., 1996). Stathmin is a regulatory protein, and its activity is regulated by phosphorylation in response to signaling or cell cycle phases (Yip et al., 2014). In Drosophila, stathmin is essential for germ cell migration and is also important in the maintenance and regulation of axonal microtubules (Duncan et al., 2013). Thymosins (spots 234 and 254) are important in the development and maintenance of the immune system (Zhang et al., 2012). Cofilin (spots 236 and 271) is fundamental for induced motility (Gurniak et al., 2005), while profilins (spots 256 and 257) have several regulatory functions in actin filament assembly and are involved in signal transduction cascades (Lu and Pollard, 2001). Tropomyosins (spots 305 and 372), identified in striated and smooth muscle, are essential for the development and body morphology of *Caenorhabditis elegans* (Anyanful et al., 2001). Actin (spots 323 and 324) has diverse physiological functions such as muscle contraction, cytoplasmic streaming, phagocytosis, morphogenetic movement, and mitosis. Kinesin 6 (spots 192

and 216) is a class of molecular motor important for intracellular transport (Shimizu et al., 2000).

4.3. Proteins related to transcription and translation function

Several proteins within the *L. apiculatum* proteomic map were identified as proteoforms related to translation and transcription such as ribosomal proteins (spots 56, 58 and 255), elongation factors (spots 62-64, 331, 345, and 346), translation initiation factors (spot 274) as well as upstream activation factor subunits (spots 327 and 328). The transcriptional activator protein Pur-alpha (spot 329) and bromodomain-containing proteins (spot 66) were also identified (**Table 1**). These proteins are emerging as being involved in adipogenesis regulation and transcriptional control (Denis et al., 2010; Wang et al., 2012). Splicing factor arginine/serine rich 7 (SFRS7, spot 237) plays an important role in regulation of gene expression. SFRS7 modulates splicing of Tau, a microtubule-associated protein in the nervous system (Burnouf et al., 2016), as well the splicing of Tau exon 10, which is a protein involved in several neurodegenerative diseases (Van Abel et al., 2011).

4.4. Protein folding, degradation, and immune proteins.

Several proteoforms of heat shock protein 70 (HSP70) and heat shock cognate protein 70 (HSC70), spots 312, 313, 314, 338, and 342 were identified. HSC70 are involved in various diseases and have become a novel target for treatment of various diseases (Liu et al., 2012). HSP60 (spots 319, 320, and 321) together with the HSP10 co-chaperone (spots 2 and 6), are important for the proper folding of mitochondrial

proteins. In *Galeruca daurica*, both HSP60 and HSP10 are expressed at all development stages and in all tissues analyzed, and both are down-regulated in the 2nd instar larvae by heat and cold stresses (Tan et al., 2017). Prefoldin (spot 363) is a molecular chaperone that acts together with other chaperonins to correctly fold of nascent proteins (Whitehead et al., 2007). On the other hand, the ubiquitin-proteasome system (UPS) is the main proteolytic pathway responsible for protein degradation (Lipinszki et al., 2013). Several UPS proteoforms were identified in *L. apiculatum* larvae (spots 83, 106, 128, 243, 311, 317, 318, and 347).

PPIases, identified in spots 22, 91, and 282, belong to the peptidyl-prolyl cis-trans isomerase family, which have a role in the folding of newly synthesizes proteins (Shaw, 2002; Zhang et al., 2013). They are classified into three distinct classes: cyclophilins, FK506-binding proteins, and parvulin-like PPIases. Cyclophilins (CYPs, spot 76) and FKBPs (spot 60) are referred to as immunophilins (He et al., 2004). Calreticulin (spot 67) is important in the folding of nascent polypeptides as well as in calcium homeostasis, signaling, apoptosis, and immune functions (Sun et al. 2017).

4.5. Cell signaling and antioxidant activity

Cell signaling related proteins such as calmodulin (spot 55) and C-type lectin (spot 100) were also identified in *L. apiculatum* larvae. Calcium signaling mediates cold sensing in insect tissues through calcium/calmodulin-dependent protein kinase II (Dodd and Drickmar, 2001; Teets et al., 2013). Peroxiredoxins (PRXs) play important roles in the insects' protection against the toxicity of reactive oxygen species (Wang et al., 2016). In *L. apiculatum* larvae proteome, the PRX-5 (spot 78) and PRX-6 (spots 229,

20

289, and 290) were detected. In Drosophila, mitochondrial PRX-5 plays an important role in the maintenance of the cellular redox state, survival and prevention of apoptosis (Radyuk et al., 2010), while PRX-6 was detected in seminal fluids in the bug *Cimex lectularius* (Reinhardt et al., 2009). 2-Cys peroxiredoxin was detected in spot 253, and PRX-1 in spot 369. 2-Cys acts as antioxidant enzyme in *Bombyx mori* (Wang et al., 2016), and PRX-1 functions to protect against oxidative stress caused by bacterial infection in *Acyrthosiphon pisum* (Zhang and Lu, 2015).

Manganese superoxide dismutase (spot 98) is a well-recognized ROS scavenger enzyme; in *Hyphantria cunea* it has been associated with stress response to heat, cold, starvation, and heavy metals (Kim et al., 2010). Phospholipid hydroperoxide glutathione peroxidases (PHGPX, spots 247 and 364) are essential cellular antioxidant defense enzyems. In *Bemisia tabaci* PHGPXs expression was increased in the larvae stage, and was higher in female than male adults (Jiu et al., 2015).

4.6. Transport and oxide-reduction processes

Myelin P2 protein-like (spots 34, 75, and 249) is an extrinsic basic protein membrane localized in the central and peripheral nervous system (Hunter et al., 2005; Maddalo et al. 2010). Electron transfer flavoprotein (ETF) is a mitochondrial matrix heterodimer with α (ETFA; 30 kDa, spot 183) and β (ETFB; 28 kDa, spots 105 and 107) subunits. Defects in EFTA and EFTB are the cause of glutaric aciduria type 2A, an inherited disorder of fatty acid, amino acid, and choline metabolism (Rosenbohm et al., 2014). The 11β-hydroxysteroid dehydrogenase type 2 (11β-HSD2, spot 128) catalyzes the inactivation of glucocorticoids. This enzyme is expressed within the placenta; its

function is to limit the passage of glucocorticoids to the fetus. The absence or down-regulation of 11β-HSD2 is associated with reduced in fetal growth and birth weight (Cottrell et al., 2014). Protein disulfide isomerase (PDI, spot 315, 316, 333, and 336) is responsible for regulating cytoskeletal reorganization by the exchange of thiol-disulfide bonds in β-actin (Soblerajska et al., 2014).

4.7. Other processes

The phosphatidylethanolamine-binding protein (PEBP, spots 23 and 230) binds phospholipids (Zhang et al., 2007). In transgenic flies, *PEBP* overexpression is associated with protection against bacterial infection (Reumer et al., 2009). Calumenin (spot 65) is a multiple EF-hand Ca^{2+}-binding protein, highly expressed during the early stage of the heart development (Lee et al., 2013). The nucleoplasmin-like, detected in spot 299, has a function in the assembly of nucleosomes (Padeken et al., 2013). Several cuticle proteoforms were identified (spots 27, 51 and 99), and together with chitin fibers, are the composite material of the extracellular matrix (Charles, 2010).

Poly(A) specific ribonuclease (PARN, spot 32), one of the most well-characterized deadenylases, is the enzyme responsible for trimming and maturation of Ago2-cleaved pre-miR-451 (Yoda et al., 2013). PARN are the major deadenylase in *Aedes albopictus*, and are part of the mRNA decay machinery (Opyrchal et al., 2005). Ferritin (spot 295) in insects works to store and transport iron, while transferrin (spots 339, 340, 341, and 343), which is present in the hemolymph, may also function as an iron transport protein (Pham and Winzerling, 2010). Hemolymph ferritin is an alternative protein for dietary iron delivery in insects, whereas in addition to the role in iron delivery, transferrin also

participates in oxidative stress reduction and to enhance insect survival to infections (Geiser and Winzerling, 2012). Several spots (129, 135, 350, 366, and 367) were identified as related to chitinase 3 and chitinase-like proteins. Chitinases are well known proteins to several functions; they are involved in digestion, arthropod molting, defense/immunity, and pathogenicity (Kock et al., 2014).

4.8. Hexamerins structure and expression along the L. apiculatum life cycle

Interest in hexamerins relates to their function as storage proteins, providing energy during non-feeding periods of ant development (Martins et al., 2010; Guo et al., 2013), but also to their versatility. Hexamerins may function in the transport of hormones (Braun and Wyatt, 1996), as well as play a role in immune response (Hakim et al., 2007; Poopathi et al., 2014). Given the critical role of hexamerins in insect development, studies concerning their structure, biosynthesis, regulation, evolution, and caste differentiation have been carried out (Cunha et al., 2005; Tsai et al., 2014; Xie and Luan, 2014; Burmester et al., 2015; Rao et al., 2016; Okada et al., 2017).

Hexamerins have diverse amino acids composition and functions (Burmester, 2015). Arylphorins are characterized by high content of Phe and Tyr (up to 25%), while others hexamerins are rich in Met (Telfer and Kunkel, 1991). The deduced LaHEX amino acid sequence (**Figure 4**) consists of high content of Gln (20.7%), Ala and Tyr (6.3 and 6.0%, respectively), as well as essential amino acids such as Lys (1.9%), Met+Cys (1.2%), His (3.3%), Phe (3%), Trp (0.4%), Leu and Ile (7.2 and 5.9%, respectively), and Val (7.8%). This composition is similar to that reported for the *Bactrocera dorsalis* hexamerin (Tsai et al., 2014). LaHEX primary protein structure

shows the conserved N, M, and C hemocyanin domains (Figure 6). Hemocyanin N contains the all-alpha domain and Hemocyanin M is described as metalloprotein containing two copper atoms, which are considered to function in oxygen transport. Hemocyanin C contains Ig-like domains and plays key roles in immune system, with antibacterial and phagocytic activities against bacteria (Zhang et al., 2009; Quin et al., 2018).

L. apiculatum is holometabolous (undergoes complete metamorphosis), with four stages of life: egg, larva, pupa, and imago or adult (Kaspari, 2003). In the Mexican Plateau, the *L. apiculatum* life cycle begins with the nuptial flight between March and April (Lara-Juárez et al., 2015). Oviposition starts two days after the flight; by the fifth day, queens place 400 to 600 eggs in their nests, eggs hatch approximately 30 days later. Larvae thicken and turn from opaque white to having clearly distinguished body segmentation. Pupas start to emerge and black points (eyes and legs) are visible. Workers and the first generation arise after 45-60 days (Ramos-Elorduy et al., 1984). Expression levels of *hemocyanin* and *LaHEX* transcripts were analyzed at different stages of ant development (egg, larvae, pupa, and adult ant, **Figure 7A**). Hemocyanin expression was similar in egg, larva, and pupa stages, but was down-regulated in adult ants (**Figure 7B**). Hexamerin was up-regulated in larval and pupa stages but down-regulated in eggs and adult ants (**Figures 7A**). This could suggest that hexamerins may serve as protein storage that is used during the metamorphosis events (Burmester, 1999, 2015).

5. Conclusions

This work presents the first 2-DE proteome map of *L. apiculatum* larvae. From the 380 protein spots analyzed, 174 were successfully identified by LC-M/MS, highlighting the accumulation of different proteoforms of several proteins including hexamerins. The analysis of *de novo* sequencing and bioinformatics resulted in identification of 36 additional protein spots, most of which were hexamerins and hemocyanins isoforms. Most identified proteins have not been described for *L. apiculatum* larvae, or had only been narrowly described in ants or other hymenopterans, but were widely described in humans, Drosophila, and *C. elegans*. Identified proteins in *L. apiculatum* proteome were related to macronutrients metabolism. Immunogenic and defense proteins such as PPIases, FKB506, PEBP, cuticle proteins, and chitinases were identified. Hexamerins were highly accumulated in *L. apiculatum* larvae and the cDNA for the most abundant was isolated and characterized. LaHEX contains the canonic N, M, and C hemocyanin domains, and is evolutionarily related to *Apis mellifera* HEX110. Our results reinforce that proteomic analysis of non-sequenced species was successful, giving valuable insight into the *L. apiculatum* larvae proteome that could help to understand their biochemistry and physiology and opening new interest in *escamolera* ants research.

Acknowledgments

Pecuaria, Acuacultura, Agrobiotecnología y Recursos Fitogenéticos, CONACYT-B-S-

3804".

Competing interests

The authors declare there are no competing interests.

References

Amore, V., Gaetini, B., Puig, M.A., Fochetti, R., 2011. New data on the presence of hemocyanin in Plecoptera: Recomposing a puzzle. J. Insect Sci. 11, 153.

Anyanful, A., Sacube, Y., Takuwa, K., Kagawa, H., 2001. The third and fourth tropomyosin isoforms of *Caenorhabditis elegans* are expressed in the Pharynx and intestines and are essential for development and morphology. J. Mol. Biol. 313, 525-537.

Bragg, J., Rajkovic, A., Anderson, C., Curtis, R., Van Houten, J., Begres, B., Naples, C., Snider, M., Fraga, D., Singer, M., 2012. Identification and characterization of a putative arginine kinase homolog from *Myxococcus xanthus* required for fruiting body formation and cell differentiation. J. Bacteriol. 194, 2668-2676.

Braun, R.P., Wyat, G.R., 1996. Sequence of the hexameri juvenile hormone-binding protein from the hemolymph of Locusta migratoria. J. Biol. Chem. 271, 31756-31762.

Bulock, K.G., Beardsley, G.P., Andersen, K.S., 2002. The kinetic mechanisms of the human bifunctional enzyme ATIC (5-amino-4-imidazolecarboxamide ribonucleotide transformylase/inosine 5´-monophosphate cyclohydrolase). J. Biol. Chem. 277, 22168-2274.

Burmester, T., 1999. Evolution and function of the insect hexamerins. Eur. J. Entomol. 96, 213-225.

Burmester, T., 2015. Expresssion and evolution of hexamerins from the tobacco hornworm, Manduca sexta, and other Lepidoptera. Insect Biochem. Mol. Biol. 62, 226-234.

Burmester, T., Hankeln, T., 2007. The respiratory proteins of insects. J. Insect Physiol. 53, 285-294.

Burnouf, S., Grönke, S., augustin, H., Dols, J., Gorsky, M.K., Werner, J., Kerr, F., Alic, N., Martinez, P., Partridge, L., 2016. Deletion of endogenous Tau protiens is not detrimental in Drosophila. Scientifc Rep. 6, 23102.

Charles, J.P., 2010. The regulation of expression of insect cuticle protein genes. Insect Biochem. Mol. Biol. 40, 205-213.

Charrier, C., Duncan, G.J., Reid, M.D., Rucklidge, G.J., Henderson, D., Young, P., Russell, V.J., Aminov, R.I., Flint, H.J., Louis, P., 2006. A novel class of CoA-

transferase involved in short-chain fatty acid metabolism in butyrate-producing human colonic bacteria. Microbiol. 152, 179-185.

Cheng, Q., Gu, Sh., Liu, Z., Wang, Ch.-Z., Li, X., 2017. Expressional divergence of the fatty acid-amino acid conjugate-hydrolyzing aminoacylase 1 (L-ACY-1) in *Helicoverpa armigera* and *Helicoverpa assulta*. Scientific Rep. 7, 87121.

Chiarelli, L.R., Morera, S.M., Bianchi, P., Fermo, E., Zanella, A., Galizzi, A., Valentini, G., 2012. Molecular insights on pathogenic effects of mutations causing phosphoglycerato kinase deficiency. PLoS One 7, e32065.

CONABIO., 2008. Himenópteros. In: S. Ocegueda and J. Llorente (eds). Catálgo taxonómico de especies de México. Concoimiento actual de la biodiversidad. CONABIO, MÉXICO.

Conesa, A., Götz, S., García-Gómez, J.M., Terol, J., Talón, M., Robles, M., 2005. Blast2GO: a universal tool for annotation, visualization and analysis in functional genomics research. Bioinformatics 21, 3674-3676.

Cottrell, E.C., Seckl, J.R., Holmes, M.C., Wyrwoll, C.S., 2014. Foetal and placental 11β-HASD2: a hub for developmental programming. Acta Physiol. 210, 288-295.

Cunha, A.D.., Nascimento, A.M., Guidugli, K.R., Simões, Z.L.P., Bitondi, M,M.G., 2005. Molecular cloning and expression of a hexamerin of cDNA from the honey bee, *Apis mellifera*. J. Insect Physiol. 51, 1135-1147.

De Morais Guedes, S., Vitorino, R., Domingues, R., Tomer, K., Correia, A.J.F., Amado, F., Domingues, P., 2005. Proteomics of immune-challenged *Drosophila melanogaster* larvae hemolymph. Biochem. Biophys. Res. Commun. 328, 106-115.

Del Toro, I., Pacheco, J.A., Mackay, W.P., 2009. Revision of the Ant Genus *Liomeopum* Mayr (Hymenoptera:Formicidae). Sociobiology 52, 299-369.

Denis, G.V., Nikolajczyk, B.S., Schnitzler, G.R., 2010. An emerging role for bromodomain-containing proteins in chromatin regulation and transcriptional control of adipogenesis. FEBS Lett. 584, 3260-3268.

Díaz-Ramos, Ám, Roig-Borrellas, A., García-Melero, A., López-Alemany, R., 2012. A-enolase, a multifunctional protein: its role on pathophysiological situations. J. Biomed. Biotechnol. 2012, 1-12.

Dodd, R.B., Drickmar, K., 2001. Lectin-like proteins in model organisms: implications for evolution of carbohydrate-binding activity. Glycobiology 11, 71R-79R.

Duncan, J.E., Lytle, N.K., Zuniga, A., Goldstein, L.S., 2013. The microtubule regulatory protein stathmin is required to maintain the integrity of axonal microtubules in Drosophila. PLoS One 26, e68324.

Eskinazi, R., Thöny, B., Svoboda, M., Robberecht, P., Dassesse, D., Heizmann, C.W., Van Laethem, J.L., Resibois, A., 1999. Overexpression of Pterin-4a-carbinolamine dehydratase/Dimerization cofactor of hepatoxyte nuclear factor 1 in human colon cancer. Am. J. Pathol. 155, 1105-1113.

FAO., 2013. Edible insects: Future prospects for food and feed security. Forestry paper, 171:1-154.

Findlay, G.D., MacCoss, M.J., Swanson, W.J., 2009. Proteomic discovery of previously unannotated, rapidly evolving seminal fluid genes in Drosophila. Genome Res.19, 886-896.

Findlay, G.D., Swanson, W.J., 2010. Protoemics enhances evolutionary and functional analysis of reproductive proteins. BioEssays 32, 26-36.

Finn, R.D., Clements, J., Arndt, W., Miller, B.L., Wheeler, T. J., Schreiber, F., Bateman, A. and Eddy, S.R., 2015. HMMER web server: 2015 update. Nucleic Acids Res. 43, W30-W38.

Fujii, T., Abe, H., Kawamoto, M., Katsuma, S., Banno, Y., Shimada, T., 2013. Albino (al) is a tetrahydrobiopterin (BH4)-deficient mutant of the silkworm *Bombyx mori*. Insect Biochem. Mol. Biol. 43, 495-600.

Geiser, D.L., and Winzerling, J.J., 2012. Insect transferrins: multifunctional proteins. Biochim. Biophys. Acta (BBA)-General Subjects, 1820, 437-451.

Gao, K., Deng, X.Y., Shang, M.K., Qin, G.X., Hou, C.X., Guo, X.J., 2017. iTRAQ-based quantitative proteomic analysis of midgut in silkworm infected with *Bombyx mori* cytoplasmic polyhedrosis virus. J. Proteomics 152, 300–311.

Guo, L., Zhao, X., Zhang, Y., Wang, Z., Zhong, M., Li, Sh., Lun, J., 2013. Evidences of SNPs in the variable region of hemocyanin Ig-like domain in shrimp *van*. Fish Shellfish Immunol. 35, 1532-1538.

Gurniak, C.B., Perlas, E., Witke, W., 2005. The actin depolymerizing factor n-cofilin is essential for neural tube morphogenesis and neural crest cell migration. Dev. Biol. 278, 231-241.

Hakim, R.S., Blackburn, M.B., Corti, P., Gelman, D.B., Goodman, C., Elsen, K., Loeb, M.J., Lynn, D., Soin, T., Smagghe, G., 2007. Growth and mitogenic effects of arylphorin *in vivo* and *in vitro*. Arch. Insect Biochem. Physiol. 64, 63-73.

He, Z., Li, L., Luan, S., 2004. Immunophilins and parvulins. Superfamily of peptiyl prolyl isomerases in Arabidopsis. Plant Physiol. 145, 1248-12467.

Horowitz, A., Clément-Chomienne, O., Walsh, M.P., Tao, T., Katsuyama, H., Morgan, K.G., 1996. Effects of calponin on force generation by single smooth muscle cells. Am. J. Physiol. Heart C 270, H1858-1863.

Huerta-Ocampo, J.A., Barrera-Pacheco, A., Mendoza-Hernández, C.S., Espitia-Rangel, E., Mock, H.-P., Barba de la Rosa, A.P., 2014. Salt Stress-Induced Alterations in the Root Proteome of *Amaranthus cruentus* L. J. Proteome Res. 13, 3607-3627.

Hunter, D.J., Macmaster, R., Roszak, A.W., Riboldi-Tunnicliffe, A., Griffiths, I.R., Freer, A.A., 2005. Structure of myelin P2 protein from equine spinal cord. Acta Crystallogr D Biol. Crystallogr. 61, 1067-1071.

Jansson, A., Berggren, A., 2015. Insects as food – Something for the future? A report from Future Agriculture. Uppsala, Swedish University of Agricultural Sciences (SLU).

Jiu, M., Li, J.M., Gao, X.L., Wang, L.J., Wang, X.W., Liu, S.S., 2015. Identification and characterization of two phospholipid hydroperoxide glutathione peroxidase genes from the Mediterranean species of the whitefly *Bemisia tabaci* complex. Arch. Insect. Biochem. Physiol. 89, 54-67.

Kaji, H., Tsuji, T., Mawuenyega, K.G., Wakamiya, A., Taoka, M., Isobe, T., 2000. Profiling of *Caenorhabditis elegans* proteins using two-dimensional gel electrophoresis and matrix assisted laser desorption/ionization-time of flight-mass spectrometry. Electrophoresis 21, 1755-1765.

Kaspari, M., 2003. Introducción a la ecología de las hormigas. In: F. Fernández (ed.). Intorducción a las hormigas de la región neotropical. Instituto de Investigación de Recursos Biológicos Alexander von Humboldt. Pp. 97-112, Bogota, Colombia.

Kim, Y.I., Kim, H.J., Kwon, Y.M., Kang, Y.J., Lee, I.H., Jin, B.R., Han, Y.S., Cheon, A.M., Ha, N.G., Seo, S.J., 2010. Modulation of MnSOD protein in response to different experimental stimulation in *Hyphantria cunea*. Comp. Biochem. Physiol. B Biochem. Mol. Biol. 157, 343–350.

Kishita, Y., Tsuda, M., Aigaki, T., 2012. Impaired fatty acid oxidation in a Drosophila model of mitochondrial trifunctional protein (MTP) deficiency. Biochem. Biophys. Res. Commun. 419, 344-349.

Kock, B.E.V., Stougaard, J., Spaink, H.P., 2014. Spatial and temporal expression patterns of chitinase genes in developing zebrafish embryos. Gene Expr. Patterns 14, 69-77.

Kuhns, E.H., Seidl-Adams, I., Tumlinson, J.H., 2012. Heliothine caterpillars differ in abudnance of a gut lumen aminoacylase (L-ACY-1)-suggesting a relationship between host preference and fatty acid amino acid conjugate metabolism. J. Insect Physiol. 58, 408-412.

Ladrón De Guevara, O., Padilla, P., García, L., Pino, J.M., Ramos-Elorduy, J., 1995. Amino acid determination in some edible Mexican insects. Amino Acids 9, 161-173.

Lara-Juárez, P., Aguirre-Rivera, J.R., Castillo-Lara, P., Reyes-Agüero, J.A., 2015. Biologia y aprovechamiento de la homiga de escamoles, *Liometopum apiculatum* Mayr (Hymenoptera:Formicidae). Acta Zoool. Mex. 31, 251-264.

Lee, J.H., Kwon, E.G., Kim, D.H., 2013. Calumenin has a role in the alleviation of ER stress in neonatal rat cardiomyocytes. Biochem. Biophys. Res. Commun. 439, 327-32.

Letunic, I., Bork, P., 2007. Interactive Tree Of Life (iTOL): An online tool for phylogenetic tree display and annotation. Bioinformatics, 23, 127–128.

Lipinszki, Z., Klement, E., Hunyadi-Gulyas, E., Medzihradszky, K.F., Márkus, R., Pál, M., Déak, P., Udvardy, A., 2013. A novel interplay between the ubiquitin-proteasome system and serine proteases during Drosophila development. Biochem. J. 454, 571-583.

Liu, H., Zeng, H., Yao, Q., Yuan, J., Zhang, Y., Qiu, D., Yang, X., Yang, H., Liu, Z., 2012. *Steinernema glaseri* surface enolase: Molecular cloning, biological characterization, and role in host immune suppression. Mol. Biochem. Parasitol. 185, 89-98.

Livak, K.J., Schmittgen, T.D., 2001. Analysis of Relative Gene Expression Data Using Real- Time Quantitative PCR and the $2^{-\Delta\Delta CT}$ Method. Methods 25, 402–408.

Lu, J., Pollard, T.D., 2001. Profilin binding to poly-L-proline and actine monomers along with ability to catalyze actin nucleotide exchange is required for viability of fission yeast. Mol. Biol. Cell 12, 1161-1175.

Mackey, A.J., Haystead, T.A.J., Pearson, W.R., 2002. Getting more from less. Algorithms for rapid protein identification with multiple short peptide sequences. Mol. Cell. Proteomics 1.2, 139-147.

Maddalo, G., Shariatgorji, M., Adamas, C.M., Fung, E., Nilsson, U., Zubarev, R.A., Sedzik, J., Llag, L.L., 2010. Porcine P2 myelin protein primary structure and bound

fatty acids determined by mass spectrometry. Anal. Bioanal. Chem. 397, 1903-1910.

Madsen, P., Kibæk, M., Roca, X., Sachidanandam, R., Krainer, A., Christensen, E., Steiner, R.D., Gibson, K.M., Corydon, T.J., Knudsen, I., Wanders, R.J.A., Ruiter, J.P.N., Gregersen, N., Andresen, B.S., 2006. Short/branched-chain acyl-CoA dehydrogenase deficiency due to an IVS3+3A>G mutation that causes exon skipping. Hum. Genet. 118, 680-690.

Magdeldin, S., Enany, Sh., Yoshida, Y., Xu, B., Zhang, Y., Zureena, Z., Lokamani, I., Yaoita, E., Yamamoto, T., 2014. Basic and recent advances of two dimensional-polyacrylamide gel electrophoresis. Clinical Proteomics 11:16.

Martins, J., Nunes, F., Cristino, A., Simoes, Z., Bitondi, M., 2010. The four hexamerin genes in the honey bee: structure, molecular evolution and function deduced from expression patterns in queens, workers and drones. BMC Mol. Biol. 11, 23.

Melo-Ruiz, V., Sánchez-Herrera, K., Sandoval-Trujillo, H., Quirino-Barreda, T., Calvo-Carrillo, C., 2013. Lipids data composition of edible ant eggs *Liometopum apiculatum* M. escamoles. J. Life Sci. 7, 547-52.

Nguyen, T.T.A., Magnoli, I., Cloutier, C., Michaud, D., Muratori, F., Hance, T., 2013. Early presence of an enolase in the oviposition injecta of the aphid parasitoid *Aphidius ervi* analyzed with chitosan beads as artificial hosts. J. Insect Physiol. 59, 11-18.

Okada, Y., Watanabe, Y., Tin, M.M.Y., Tsuji, K., Mikheyev, A.S., 2017. Social dominance alters nutrition-related gene expression immediately: transcriptomic evidence from a monomorphic queenless ant. Molecular Ecol. 26, 2922-2938.

Oliveira, B.M., Coorssen, J.R., Martins-de-Souza, D., 2014. 2DE: The phoneix of proteomics. J. Proteomics 104, 140-150.

Opyrchal, M., Anderson, J.R., Sokoloski, K.J., Wilusz, C.J., Wilusz, J., 2005. A cell-free mRNA stability assay reveals conservation of the enzymes andmechanisms of mRNA decay between mosquito and mammalian cell lines. Insect Biochem. Mol. Biol. 35, 1321-1334.

Padeken, J., Mendiburo, M.J., Chlamydas, S., Schwarz, H.J., Kremmer, E., Heun, P., 2013. The nucleoplasmin homolog NLP mediates centromere clustering and anchoring to the nucleolus. Mol. Cell 50, 236-249.

Parkhitko, A.A., Binari, R., Zhang, N., Asara, J.M., Demontis, F., Perrimon, N., 2016. Tissue-specific down-regulation of S-adenosyl-homocysteine via suppression of dAhCyL1/dAhcyL2 extends health span and life span in Drosophila. Genes Dev. 30, 1409-1422.

Pearson, W.R., 2000. Flexible sequence similarity searching with the FAST3 program package. Methods Mol. Biol. 132, 185-219.

Pham, D.Q.D., Winzerling, J.J., 2010. Insect ferritins: Typical or atypical? Biochim. Biophys. Acta 1800, 824-833.

Pomastowski, P., Buszewski, B., 2014. Two-dimensional gel electrophoresis in the light of new developments. Trends Anal. Chem. 53, 167-177.

Poopathi, S., Thirugnanasambantham, K., Mani, C., Mary, K.A., Mary, B.A., Balagangadharan, K., 2014. Hexamerin a anovel protein associated with Bacillus sphaericus resistnace in Culex quinquefasciatus. Appl. Biochem. Biotechnol. 172, 2299-2307.

Quin, Z., Babu, V.S., Wan, Q., Muhammad, A., Li, J., Lan, J., Lin, L., 2018. Antibacterial activity of hemocyanin from red swamp crayfish (*Procambarus clarkii*). Fish Shelfish Immunol. 75, 391-399.

Radyuk, S.N., Rebrin, I., Klichko, V.I., Sohal, B.H., Michalak, K., Benes, J., Sohal, R.S., Orr, W.C., 2010. Mitochondrial peroxiredoxins are critical for the maintenance of redox state and the survival of adult Drosophila. Free Radical Biol. Med. 49, 1892–1902.

Ramos-Elorduy, J., Pino, M., 2003. El consumo de insectos entre los aztecas. Conquista y Comida: consecuencias del Encuetnro de Dos Mundos. (ed. J. Longs), pp. 89-101. Universidad Nacional Autónoma de México, Mexico D.F.

Ramos-Elorduy, J., Pino, J.M., 2003. El consumo de insectos entre los aztecas. Conquista y Comida: Consecuencias del Encuentro de Dos Mundos. Universidad Nacional Autónoma de México, Mexico D.F. pp. 89-101.

Ramos-Elorduy, J., Pino, J.M., Martínez, V.H.C., 2008. Una vista a la biodiversidad de la antropoentomofagía mundial. Entomol. Mex. 7, 308-313.

Ramos-Elorduy, J., Pino, J.M., Morales De León, J., 2002. Análisis químico proximal, vitaminas y nutrimentos inorgánicos de insectos consumidos en el estado de Hidalgo, México. Folia Entomol. Mexi. 41, 5-29.

Ramos-Elorduy de Conconi, J., Délage-Darchen, B., Cuadriello-Aguilar, J.I., Galindo-Miranda, N., Pino-Moreno J.M., 1984. Ciclo de vida y fundacion de las sociedades de Liometopum apiculatum M. (Hymenoptera, Formicidae). Ser. Zool. 1, 161-176.

Ramos-Elorduy, J., Levieux, J., 1992. *Liometopum apiculatum* Mayr and L. occidentale Wheeler foraging areas studied with radio-isotopes markers (Hymenoptera, Formicidae-Dolichoderinae). Bull. Soc. Zoologique France, 117, 21-30.

Ramos-Rostro, B., Quintero Salazar, B., Ramos-Elorduy, J., Pino Moreno, J.M., Ángeles Campos, S.C., García Pérez, Á., Barrera García, V.D., 2012. Análisis químico y nutricional de tres insectos comestibles de interés comercial en la zona arqueológica del municipio de San Juan Teotihuacán y en Otumba, en el estado de México. Interciencia, 37, 914-920.

Rao, V.V., Ningshen, T.J., Chaitanya, R.K., Senthikumaran, B., Dutta-Gupta, A., 2016. Cloning and characterization of a riboflavin-binding hexamerin form the larval fat body of a lepidopetran stored grain pest. Corcyra cephalonica. Comp. Biochem. Physiol. B Biochem. Mol. Biol.194-195, 58-64.

Reinhardt, K., Wong, C.H., Georgiou, A.S., 2009. Detection of seminal fluid proteins in the bed bug, *Cimex lectularius*, using two-dimensional gel electrophoresis and mass spectrometry. Parasitol. 136, 283-292.

Reumer, A., Bogaerts, A., Van Loy, T., Husson, S.J., Temmerman, L., Choi, C., Clynen, E., Hassan, B., Schoofs, L., 2009. Unraveling the protective effect of a Drosophila phosphatidylethanolamine-binding protein upon bacterial infection by means of proteomics. Dev. Comp. Immunol. 33, 1186-1195.

Rosenbohm, A., Süssmuth, S.D., Kassubek, J., Müller, H.P., Pontes, C., Abicht, A., Bulst, S., Ludolph, A.C., Pimkhardt, E., 2014. Novel ETFDH mutation and imaging findings in an adult with glutaric aciduria type II. Muscle Nerve 49, 446-450.

Rozen, S., Skaletsky, H., 2000. Primer3 on the WWW for general users and for biologist programmers. Methods Mol. Biol. 132, 365-386.

31

Shaw, P.E., 2002. Peptidyl-prolyl isomerases: a new twist to transcription. EMBO Rep. 3, 521–526.

Shimizu, T., Thorn, K., Ruby, A., Vale, R.D., 2000. ATPase kinetic characterization and single molecule behavior of mutant human kinesin motors defective in microtubule-based motility. Biochem. 39, 5265-5273.

Sinha, D.K., Atray, I., Bentur, J.S., Nair, S., 2012. Expression of *Orseolia oryzae* nucleoside diphosphate kinase (OoNDPK) is enhanced in rice gall midge feeding on susceptible rice hosts and its over-expression leads to salt tolerance in Escherichia coli. Insect Mol. Biol. 21, 593-603.

Soblerajska, K., Zkurzynski, Z., Stasiak, M., Kryczka, J., Cierniewski, C.S., Swiatkowska M., 2014. Protein disulfide isomerase directly interacts with β-actin Cys374 and regulates cytoskeleton reorganization. J. Biol. Chem. 289, 5758-5773.

Sterkel, M., Oliveira P.L., 2017. Development roles of tyrosine metabolism enzymes in the blood-sucking insect Rhodnius prolixus. Proc. R. Soc. B 284, 20162607.

Sun, J., Mu, H., Dai, K., Yi, L., 2017. Calreticulin: a potential anti-cancer therapeutic target. Pharmazie, 17, 503-510.

Tan, Y., Zhang, Y., Huo, Z.-J., Zhou, X.-R., Pang, B.-P., 2017. Molecular cloning of heat shock protein 10 (Hsp10) and 60 (Hsp60) cDNAs from *Galeruca daurica* (Coleoptera:Chrysomelidae) and their expression analysis. Bull. Entomol. Res. 1-13.

Teets, N.M., Yi, S.X., Lee, R.E., Denlinger, D.L., 2013. Calcium signaling mediates cold sensing in insect tissues. Proc. Natl. Acad. Sci. USA 110, 9154-9159.

Telfer, W.H. and Kunkel, J.G., 1991. The function and evolution of insect storage hexamers. Annu. Rev. Entomol. 36:205-228.

Tsai, M.-Ch., Tsai, Ch.-L., Chen, M.-E., 2014. cDNA cloning and transcriptional expression profiles of a hexamerin in the original fruit fly, *Bactrocera dorsalis*. Arch. Insect Biochem. Physiol. 86, 180-191.

Van Abel, D., Hölzel, D.R., Jain, S., Lun, F.M.F., Zheng, Y.W.L., Chen, E.Z., Sun, H., Chiu, R.W., Lo, Y.M., Van Dijk, M., Oudejans, C.V., 2011. SFRS7-mediated splicing of tau exon 10 is directly regulated by STOX1A in glial cells. PLoS One 6, e21994.

van Huis, A., Van Itterbeeck, J., Klunder, H., Mertens, E., Halloran, A., Muir, G., Vantomme, P., 2013. Edible insects: Future prospects for food and feed security. FAO FORESTRY PAPER 171. (ed. F.A.A.O.O.T.U. Nationss), Food and Agriculture Organization of the United Nations, Rome, Italy.

Vyatkina, K., 2017. De novo sequencing of top-down tandem mass spectra: A next step towards retrieving a complete protein squence. Proteomes 5, 6.

Wang, R., Li, R., Helfer, C.M., Jiao, J., You, J., 2012. Bromodomain Protein Brd4 Associated with Acetylated Chromatin Is Important for Maintenance of Higher-order Chromatin Structure. J. Biol. Chem. 287, 10738-10752.

Ward, P.S., Brady, S.G., Fischer, B.L., Schultz, T.R., 2010. Phylogeny and biogeography of dolichoderine ants: effects of data partitioning and relict taxa on historical inference. Syst. Biol. 59, 342-362.

Wang, Q., Zhou, Y., Chen, K., Ju, X., 2016. Identification and characterization of an atypical 2-cys peroxiredoxin from the silkworm, *Bombyx mori*. Insect Mol. Biol. 25, 347-354.

Wei, D., Zhang, M.Y., Gu, P.M., Smagghe, G., Wang, J.J., 2018. Label-free based quantitative proteomic analysis identifies protiens involved in the testis maturation of *Bactrocera dorsalis* (Hendel). Comp. Biochem. Physiol. Part D Genomics Proteomics 25, 9-18.

Whitehead, T.A., Boonyaratanakornkit, B.B., Höllrigl, V., Clark, D.S., 2007. A filamentous molecular chaperone of the prefoldin family from the deep-sea hyperthermophile *Methanocaldococcus jannaschii*. Protein Sci. 16, 626-634.

Wu, Q.Y., Li, F., Wang, X.Y., 2008. Evidence that amino-acid residues are responsible for substrate synergism of locust arginine kinase. Insect Biochem. Mol. Biol. 38, 59–65.

Xia, J.X., Guo, Z.J., Yang, Z.Z., Zhu, X., Kang, S., Yang, X., Yang, F.S., Wu, Q.J., Wang, S.L., Xie, W., Xu, W.J., Zhang, Y.J., 2016. Proteomics-based identification of midgut proteins correlated with Cry1Ac resistance in *Plutella xylostella* (L.). Pestic. Biochem. Physiol. 132, 108–117.

Xie, W., Luan, Y.-X., 2014. Evolutionary implications of dipluran hexamerins. Insect Biochem. Mol. Biol. 46, 17-24.

Yip, Y.Y., Yeap, C., Bogoyevitch, M.A., Ng, D.C.H., 2014. cAMP-dependent protein kinase and c-Jun N-terminal kinase mediate stathmin phosphorylation for the maintenance of interphase microtubules during osmotic stress. J. Biol. Chem. 289, 2157-2169.

Yoda, M., Cifuentes, D., Izumi, N., Sakaguchi, Y., Suzuki, T., Giraldez, A.J., Tomari, Y., 2013. PARN mediates 3´-end trimming of Argonaute2-cleavfed precursor micro RNAs. Cell Rep. 5, 715-726.

Zhang, G.F., Kombu, R.S., Kasumov, T., Han, Y., Sadhukhan, S., Zhang, J., Sayre, L.M., Ray, D., Gibson, K.M., Anderson, V.A., Tochtrop, G.P., Brunengraber, H., 2009. Catabolism of 4-hydroxyacids and 4-hydroxynonenal via 4-hydroyx-4-phosphoacyl-CoAs. J. Biol. Chem. 284, 33521-33534.

Zhang, Y., Lu, Z., 2015. Peroxiredoxin 1 protects the pea aphid Acyrthosiphon pisum from oxidative stress induced by Micrococcus luteus infection. J. Invertebr. Pathol. 127, 115-121.

Zhang, W., Zhang, C., Lv, Z., Fang, D., Wang, D., Nie, Z., Yu, W., Lan, H., Jiang, C., Zhang, Y., 2012. Molecular characterization, tissue distribution, subcellular localization and actin-sequestering function of a thymosin protein from silkworm. PLoS One 7, e31040.

Zhang, Y., Wang, X., Xiang, Z., Li, H., Qiu, J., Sun, Q., Wan, T., Li, N., Cao, X., Wang, J., 2007. Promotion of cellular migration and apoptosis resistance by a mouse eye-specific phosphatidylethanolamine-binding protein. Int. J. Mol. Med. 19, 55-63.

Zhang, Y., Yan, F., Hu, Zh., Zhao, X., Min, Sh., Du, Zh., Zhao, Sh., Ye, X., Li, Y., 2009. Hemocyanin from shrimp *Litopenaeus vannamei* shows hemolytic activity. Fish & Shelfish Immunol. 27, 330-335.

Zhang, Y.L., Xue, R.Y., Cao, G.L., Zhu, Y.X., Pan, Zh., Gong, C.L., 2013. Shotgun proteomic analysis of wing discs from the domesticated silkworm (*Bombyx mori*) during metamorphosis. Amino Acids 45, 1231-1241.

Figure Legends

Figure 1. Composed proteomic 2-DE map of *Liometopum apiculatum* Mayr larvae. In the first dimension (IEF), proteins were separated on 24 cm IPG strips with a linear gradient of pH 3-10 and 5-8 to obtain better resolution. In the second dimension, 13% SDS-PAGE gels were used. The most intense protein spots were cut from three different gels and analysed by LC-MS/MS.

Figure 2. Representative MS/MS analysis. Cu-Zn superoxide dismutase peptide identification by *de novo* sequencing and FASTA homology-based search. (A) Tandem mass spectrum of the *de novo* sequenced peptide, TLVLHADPDDLGQGGHELSK, using ProteinLynx Global Server. (B) Local alignment of the novo sequenced peptide with Cu-Zn superoxide dismutase through FASTA algorithm.

Figure 3. Gene ontology annotation of *Liometopum apiculatm* Mayr larvae proteins identified by LC-MS/MS and database search. Proteins were classified into categories according to Gene Ontology by using Blast2GO v3.0.8. (A) Molecular function, (B) Cellular transport, and (C) Biological processes. Proteins with multiple proteoforms were considered as one protein.

Figure 4. *Liometopum apiculatum* larvae deduced hexamerin amino acid sequence. Hemocyanin N domain is underlined; hemocyanin M domain is double underlined, hemocyanin C is underlined with dashed lines. Asterisks above letter indicate the putative phosphorylation sites (NetPhos at exapsy,org).

Figure 5. Phylogeny of 23 insect species representing five orders and crustaceus based on hexamerin storage proteins sequences. The phylogenetic tree was constructed using the Jones–Thornton–Taylor (JTT). Maximum likelihood tree was built to estimate distance and based on a Bootstrap method with at least 1000 repetitions. The circular phylogenetic tree was done using the online Interactive Tree of Life resource.

Figure 6. *Liometopum apiculatum* hexamerin showing the hemocyanin domains and compared with hexamerins from *Apis mellifera* HEX110, HEX70a,b,c. Sequence features were obtained using the HMMER biosequence analysis (https://www.ebi.ac.uk/Tools/hmmer/) which uses profile hidden Markov Models.

Figure 7. Relative expression of hemocyanin and hexamerin transcription determined by qRT-PCR. A) Developmental stages of *Liometopum apiculatum:* eggs, larva, pupa, and adult ant. B) *hemocyanin* amplification, and C) *LaHEX* amplification. Bars represent the mean of triplicates ±SD. Bars with different are significantly different at P<0.05.

Figure 1

Figure 2.

A

Precursor mass 701.3617, charge 3
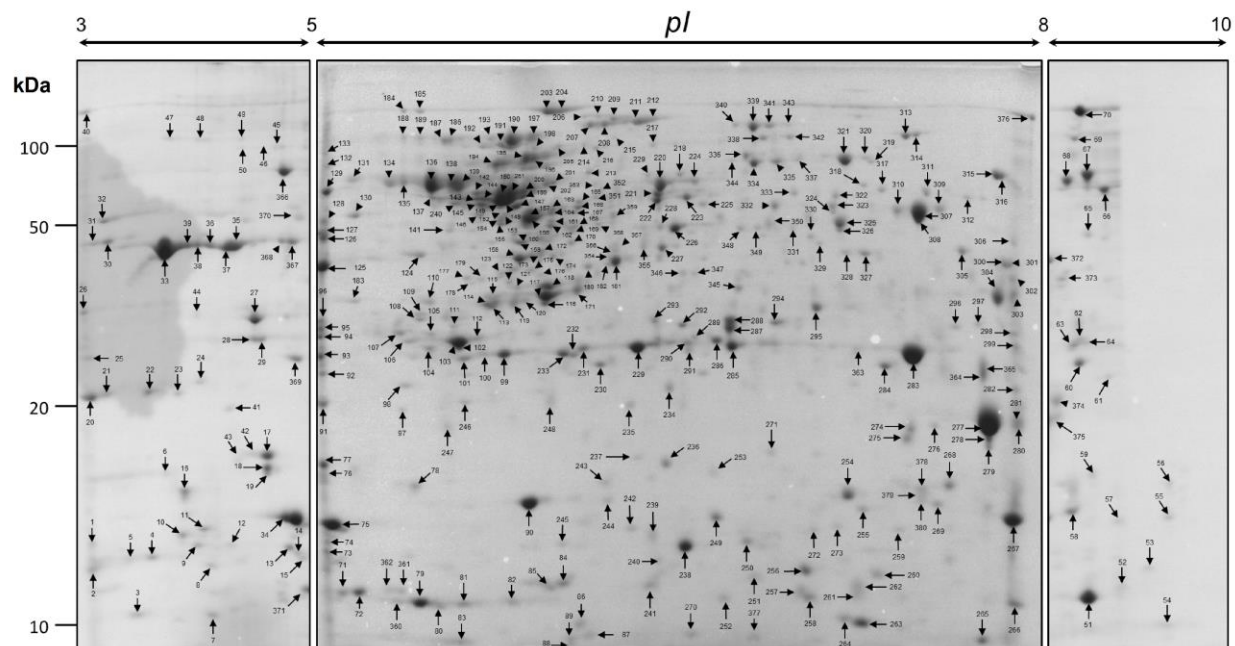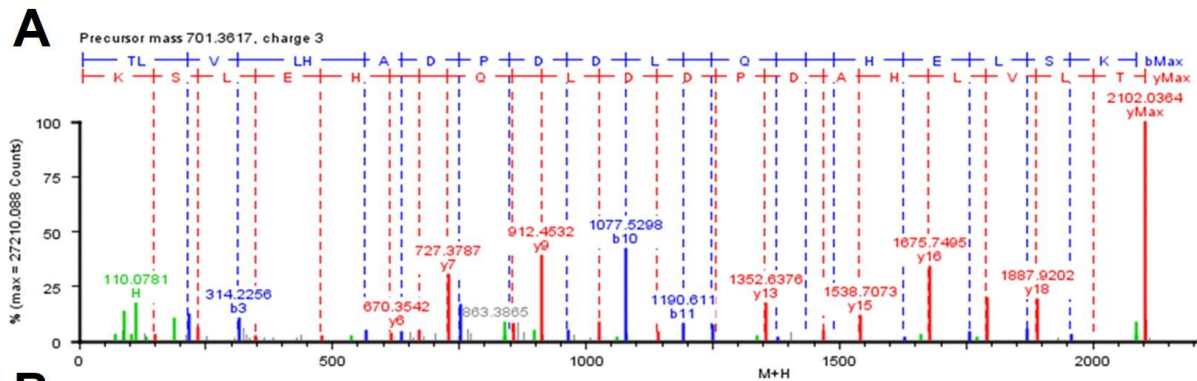
B

Spot 90

```
>>TR:E2BMV6_HARSA E2BMV6 Superoxide dismutase [Cu-Zn]
(Fragment) OS=Harpegnathos saltator OX=610380 GN=EAI_10388
PE=4 SV=1 (136 aa)
initn: 133 init1: 133 opt: 133 Z-score: 268.1  bits: 52.6 E(112022089): 4.5e-05
Smith-Waterman score: 133; 95.0% identity (100.0% similar) in 20 aa overlap (1-20:97-116)

                                        10        20
                              TLVLHADPDDLGQGGHELSK
                              :::.::::::::::::::::
TR:E2B NVEADANGVAKVNITDSIIQLCGPHSIIGRTLVVHADPDDLGQGGHELSKTTGNAGARLA
          70        80        90       100       110       120

TR:E2B CGVIGITKAQ
          130
```

Figure 3
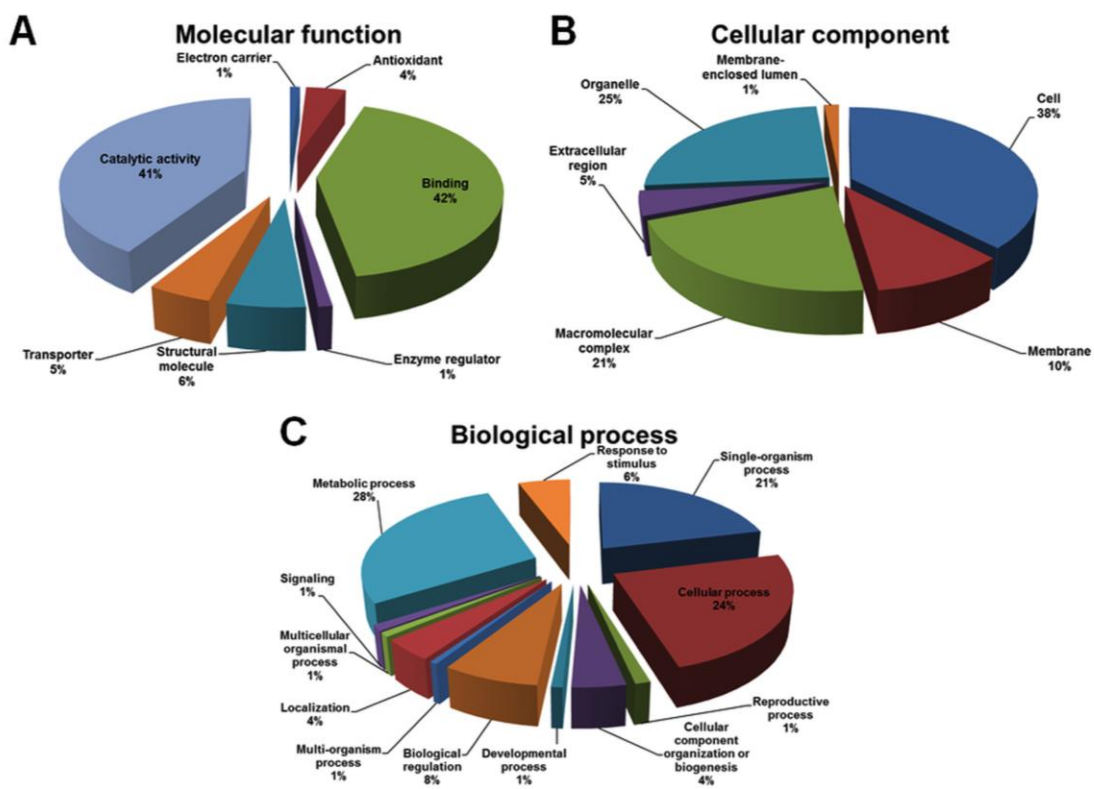
Figure 4

```
        10        20        30        40    *   50        60
QNLLGAKNYQ TLLATAAWAR VHVNEGQFVK AFIAAVLQHP ETQGIIVPSA YEIDPQLYFD

        70    *   80        90    *  100    *  * 110       120
ARIIQEAQNI AAQGSQDQVG HQQSVVIPVN YTATLPDDEQ QLSYFTQDIG LANYYAFVNL

       130 *      140    *  * 150   *    160        170 *     180
AGYFLPQQQQ TPVQYQQQQN VHSQESQTGQ GSLYYYLNQQ LLAHYELNRL TNGLGPIKDT

       190       200 *     210       220       230     * 240
DFVNVQAPYQ PHSRQINGLQ SPGRPDNLHL APANNQLIQT VMKLEQRLVE AIDSGYVITP

     * 250       260   *  * 270   *    280       290   * 300
QGAFLSLYQP QGLDILGDLI QGTGRSVNPR YYGSLQAAAC QLLGNAPQVQ NIYDYTPSVL

       310       320       330   *    340       350 *     360
ELGQVAVRDP AFYQLYKKVI QLFQHYQNSL PAYQYNDLVL PGVTIQNVQI SPFVTFFNDY
                                      ================================

   *   370       380    *  390   *    400       410       420
YVHLDNAVQQ PINNNQQQQV QQQTQPLQQQ IHSQQWQQQV QQQQQQQQQQ QHIKAQVKRL
================================================================

       430       440       450   *    460       470   *    480
DHQPYEYVIT VQSEQNIPGA VVRVYLGPKY DYQGKPVSIS QHRHQFVELD QFITDLEQGQ
================================================================

     490      500       510       520       530       540
NIINRQSQQA SGQSFDYPSI QQIQQNINSA TQPGTFYITE PHQIFGFPAR LALPKGQPQG
  * 490    *  500     *                  *
=================================================================

       550       560       570       580   *  590   *    600
VPLQLLVMIS QPEQLNVPYG PVIPEQIQTF QQHMYQVADS AEYSSQIQQQ SGKHVGVSQT
                                                    *    * *
==============================

       610   *   620       630       640   *   650       660
VEVMPENAQQ NSQAMRNQYA NLYTQQHGQY PYTHGHYQVG QTTGQGQVQG QNAWSIQNVQ

   *   670       680   *   690       700       710       720
GQHSQGQQGQ QDNIIDVQGV PASVQDMQQG MQQGAQQGAQ GVQGIQVGQG VHGIYGLQGM

       730   *
DFGGQHGFKG KYH
```
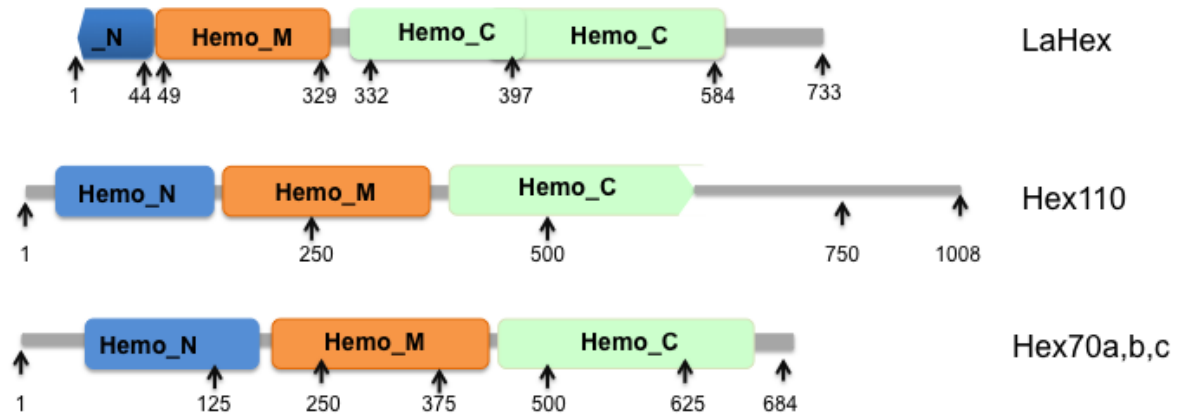
Figure 5

Figure 6

Figure 7
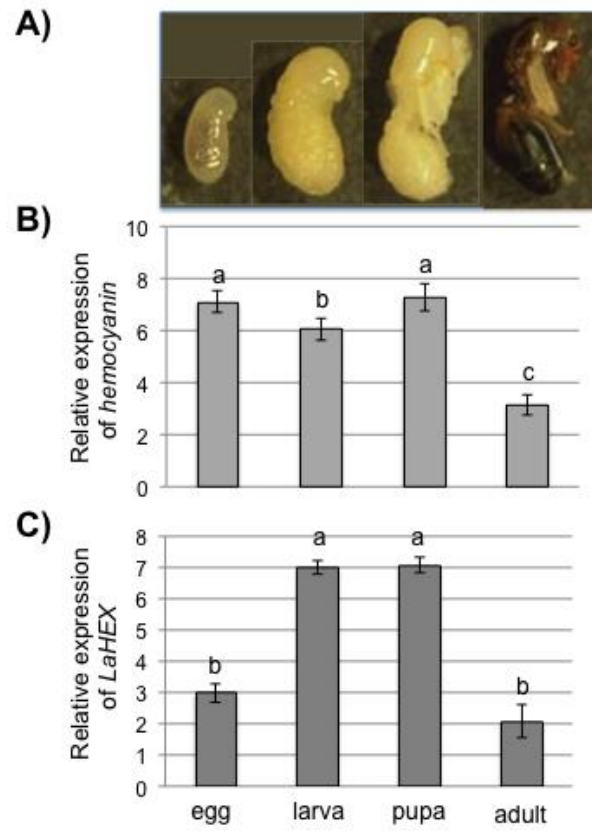
Table 1. *Liometopum apiculatum* larvae proteins spots analyzed by LC-MS/MS and identified against the *Hymenoptera* subset of the NCBInr protein database.

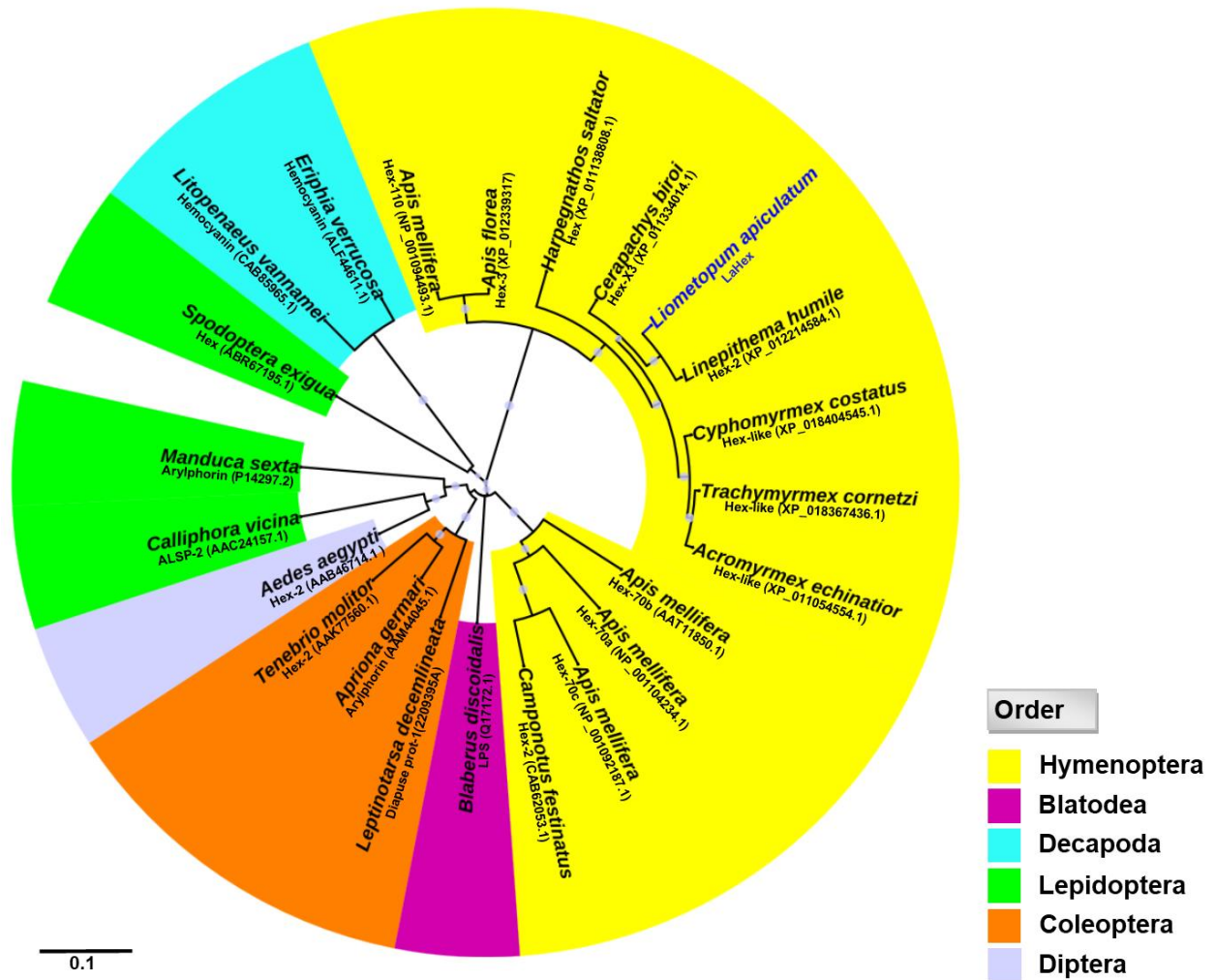| Spot No. [a]	Protein [b]	Organism	Accession number [c]	Exper. MW/*pI* [d]	Theor. MW/*pI* [e]	Mascot score [f]	Peptides /Sequence coverge (%)
Cell structure							
(24)	Myophilin	*Harpegnathos saltator*	gi|307212199	25.9/4.24	15.6/9.05	102	1/12
177	Stathmin-4	*Acromyrmex echinatior*	gi|332018661	41.2/5.63	34.9/9.44	277	4/13
214	Actin-interacting protein 1	*Acromyrmex echinatior*	gi|332023261	97.9/6.10	70.2/6.32	336	4/10
234	Thymosin beta-4	*Camponotus floridanus*	gi|307189411	22.6/6.43	18.4/5.90	121	3/17
236	Cofilin/actin-depolymerizing factor-like protein	*Camponotus floridanus*	gi|307187751	17.1/6.40	19.6/8.50	136	4/27
254	Thymosin beta-4	*Camponotus floridanus*	gi|307189411	15.7/7.21	18.4/5.90	138	4/28
256	Profilin	*Camponotus floridanus*	gi|307173635	12.0/7.04	13.9/5.65	140	2/20
257	Profilin	*Acromyrmex echinatior*	gi|332028899	11.1/7.02	20.3/9.54	44	1/12
271	Cofilin/actin-depolymerizing factor-like protein	*Camponotus floridanus*	gi|307187751	17.7/6.90	19.6/8.50	291	4/30
305	Tropomyosin 1 isoform B	*Nasonia vitripennis*	gi|229577296	45.6/7.71	32.7/4.73	359	3/10
323	Actin, clone 403	*Harpegnathos saltator*	gi|307195447	59.8/7.15	42.3/5.37	45	1/2
324	Actin, clone 403	*Acromyrmex echinatior*	gi|332024486	56.8/7.15	42./5.29	39	2/8
372	Tropomyosin-1	*Harpegnathos saltator*	gi|307196973	45.2/8.00	32.3/4.72	262	4/18
Transcription and translation							
(27)	Phosphoglycerate mutase 1	*Harpegnathos saltator*	gi|307203820	34.5/4.78	28.7/7.77	133	7/27
56	60S acidic ribosomal protein P1	*Harpegnathos saltator*	gi|307212258	16.3/9.65	13.3/4.53	96	4/46
58	Hypothetical protein SINV_06628 (60S acidic ribosomal protein P2-like)	*Solenopsis invicta*	gi|322795701	14.9/8.29	11.9/4.77	120	3/31
62	Elongation factor 1-beta'	*Camponotus floridanus*	gi|307170891	30.7/8.32	24.3/4.63	65	1/6
63	Elongation factor 1-beta'	*Camponotus floridanus*	gi|307170891	30.1/8.29	24.3/4.63	76	2/9
64	Elongation factor 1-beta'	*Harpegnathos saltator*	gi|307215145	31.4/8.40	24.3/4.72	70	2/7
66	Hypothetical protein SINV_02215 (Bromodomain-containing protein 8)	*Solenopsis invicta*	gi|322799152	64.0/8.73	125/4.81	30	1/1
68	Mitochondrial ribonuclease P protein 1 homolog	*Nasonia vitripenis*	gi|156551453	66.9/8.24	52.7/9.25	39	1/2
94	Phosphoglycerate mutase 1	*Harpegnathos saltator*	gi|307203820	31.4/5.01	28.7/7.77	150	4/16
(146)	Hypothetical protein SINV_08663	*Solenopsis invicta*	gi|322791271	55.0/5.68	51.7/8.17	297	6/13

Spot No. [a]	Protein [b]	Organism	Accession number [c]	Exper. MW/*pI* [d]	Theor. MW/*pI* [e]	Mascot score [f]	Peptides matched /Sequence coverge
	(Phosphoglycerate kinase)						
237	Splicing factor, arginine/serine-rich 7	*Camponotus floridanus*	gi|307180295	17.5/6.32	17.8/8.73	94	2/13
255	40S ribosomal protein S12	*Camponotus floridanus*	gi|307187759	15.1/7.27	15.6/5.47	86	2/19
274	Eukaryotic translation initiation factor 5A	*Camponotus floridanus*	gi|307180081	18.8/7.47	18.05/07	97	2/14
327	Upstream activation factor subunit spp27	*Acromyrmex echinatior*	gi|332018104	45.4/7.28	37.2/8.91	87	2/8
328	Upstream activation factor subunit UAF30	*Harpegnathos saltator*	gi|307214555	45.5/7.20	34.3/8.42	43	3/8
(329)	Transcriptional activator protein Pur-alpha	*Camponotus floridanus*	gi|307190558	46.6/7.09	33.7/6.86	214	5/21
331	Elongation factor 2	*Camponotus floridanus*	gi|307170298	49.6/6.98	94.3/6.11	164	4/6
345	Elongation factor 1 alpha	*Bombus mendax*	gi|27501884	39.3/6.76	42.5/8.42	58	2/2
346	Elongation factor 1 alpha	*Bombus mendax*	gi|27501884	42.1/6.52	42.5/8.42	41	2/2
(348)	Phosphoglycerate kinase	*Camponotus floridanus*	gi|307177429	48.6/6.77	45.0/6.16	393	6/16
Metabolism and energy production							
17	Nucleoside diphosphate kinase	*Harpegnathos saltator*	gi|307193761	18.4/4.88	17.4/7.79	67	1/7
(33)	Glyceraldehyde-3-phosphate dehydrogenase 2	*Acromyrmex echinatior*	gi|332026368	47.6/3.89	37.6/8.15	39	5/10
36	Glyceraldehyde-3-phosphate dehydrogenase 2	*Acromyrmex echinatior*	gi|332026368	48.8/4.33	37.6/8.15	97	8/30
(38)	Hypothetical protein SINV_01281 (Glyceraldehyde-3-phosphate dehydrogenase)	*Solenopsis invicta*	gi|322794747	48.9/4.21	74.1/6.72	151	6/9
(39)	Hypothetical protein SINV_01281 (Glyceraldehyde-3-phosphate dehydrogenase)	*Solenopsis invicta*	gi|322794747	48.7/4.08	74.1/6.72	146	6/9
42	Nucleoside diphosphate kinase	*Camponotus floridanus*	gi|307173082	18.6/4.76	19.6/8.41	30	1/4
(45)	Hypothetical protein SINV_11660(Bifunctional purine biosynthesis protein PURH)	*Solenopsis invicta*	gi|322795791	93.9/5.02	65.2/7.58	62	2/4
46	Hypothetical protein SINV_11660(Bifunctional purine biosynthesis protein PURH)	*Solenopsis invicta*	gi|322795791	93.0/4.96	65.2/7.58	46	2/4
77	Nucleoside diphosphate kinase	*Harpegnathos saltator*	gi|307193761	17.0/5.02	17.4/7.79	45	2/13
79	Pterin-4-alpha-carbinolamine dehydratase 2	*Acromyrmex echinatior*	gi|332030543	10.6/5.43	15.7/9.67	34	4/17

44

Spot No. [a]	Protein [b]	Organism	Accession number [c]	Exper. MW/pI [d]	Theor. MW/pI [e]	Mascot score [f]	Peptides matched /Sequence coverge
81	Pterin-4-alpha-carbinolamine dehydratase 2	*Harpegnathos saltator*	gi|307206440	10.5/5.61	15.5/9.72	100	1/11
(100)	Triosephosphate isomerase	*Acromyrmex echinatior*	gi|332024520	28.9/5.69	26.9/7.71	57	2/9
101	Triosephosphate isomerase	*Acromyrmex echinatior*	gi|332024520	27.8/5.62	26.9/7.71	353	4/22
110	Fumaryl acetoacetate hydrolase domain-containing protein 2A	*Camponotus floridanus*	gi|307173208	36.9/5.47	36.5/8.81	89	2/7
124	Malate dehydrogenase, cytoplasmic	*Camponotus floridanus*	gi|307166391	45.2/5.43	39.2/7.03	354	5/21
(125)	Glyceraldehyde-3-phosphate dehydrogenase 2	*Acromyrmex echinatior*	gi|332026368	43.3/5.02	37.6/8.15	325	3/18
126	Fructose-bisphosphate aldolase isoform A	*Nasonia vitripennis*	gi|283046761	47.3/5.02	39.8/6.67	165	2/8
(127)	3-ketoacyl-CoA thiolase, mitocondrial	*Camponotus floridanus*	gi|307172623	47.9/5.02	42.3/8.18	152	2/3
(127)	Fructose-bisphosphate aldolase	*Acromyrmex echinatior*	gi|332021262	47.9/5.02	40.4/8.05	75	2/9
(129)	Hypothetical protein SINV_08923 (ATP synthase subunit alpha, mitochondrial)	*Solenopsis invicta*	gi|322785985	70.0/5.03	59.3/9.04	116	4/11
(129)	PREDICTED: chitinase-like protein Idgf4-like	*Apis mellifera*	gi|66514614	70.0/5.03	49.0/8.06	116	2/6
135	PREDICTED: chitinase-like protein Idgf4-like	*Apis mellifera*	gi|66514614	75.0/5.37	49.0/8.06	94	1/3
(140)	4-hydroxybutyrate coenzyme A transferase	*Acromyrmex echinatior*	gi|332024913	62.9/5.58	53.3/7.95	160	3/9
(140)	Putativeenolase	*Aphidius ervi*	gi|261259780	62.9/5.58	47.2/5.93	65	1/3
(146)	Putative enolase	*Aphidius ervi*	gi|261259780	55.0/5.68	47.2/5.93	35	1/3
147	Putative enolase	*Aphidius ervi*	gi|261259780	59.1/5.81	47.25.93	238	4/17
158	PREDICTED: enolase-like	*Megachile rotundata*	gi|383859649	44.7/5.83	47.2/6.13	153	2/8
198	PREDICTED: kinesin 6[a]	*Apis mellifera*	gi|328782772	96.6/5.90	97.5/9.17	30	1/1
199	Putative enolase	*Aphidius ervi*	gi|261259780	67.1/5.84	47.2/5.93	77	1/3
216	PREDICTED: kinesin 6[a]	*Apis mellifera*	gi|328782772	82.2/6.12	97.5/9.17	31	1/1
222	Hypothetical protein SINV_00964 (Aminoacylase-1)	*Solenopsis invicta*	gi|322800154	64.2/6.38	45.9/5.40	69	1/2
223	Hypothetical protein SINV_00964 (Aminoacylase-1)	*Solenopsis invicta*	gi|322800154	66.0/6.53	45.9/5.40	146	2/6
232	Triosephosphate isomerase	*Acromyrmex echinatior*	gi|332024520	28.6/6.06	26.9/7.71	100	3/17
233	Triosephosphate isomerase	*Acromyrmex echinatior*	gi|332024520	28.7/6.01	26.9/7.71	188	3/17
292	Pyruvate dehydrogenase	*Camponotus*	gi|30717804	33.2/6.5	38.5/5.8	62	1/4

Spot No. [a]	Protein [b]	Organism	Accession number [c]	Exper. MW/pI [d]	Theor. MW/pI [e]	Mascot score [f]	Peptides matched /Sequenc
	E1 componentsubunit beta, mitocondrial	*floridanus*	9	1	7		
297	6-phosphogluconolactonase	*Camponotus floridanus*	gi|307185950	33.3/7.78	27.2/4.95	86	2/7
(317)	ATP synthase subunit beta, mitochondrial	*Camponotus floridanus*	gi|307181472	71.3/7.35	55.1/5.33	452	7/16
(329)	Homocysteine S-methyltransferase	*Harpegnathos saltator*	gi|307193338	46.6/7.09	36.0/5.72	198	2/9
(350)	Putative chitinase 3	*Acromyrmex echinatior*	gi|332027352	51.3/6.88	33.9/5.36	61	2/9
360	Pterin-4-alpha-carbinolamine dehydratase 2	*Acromyrmex echinatior*	gi|332030543	10.7/5.35	15.7/9.67	127	2/18
366	PREDICTED: chitinase-like protein Idgf4-like	*Apis mellifera*	gi|66514614	70.0/5.03	49.0/8.06	141	2/6
367	PREDICTED: chitinase-like protein Idgf4-like	*Apis mellifera*	gi|66514614	49.6/5.05	49.0/8.06	43	1/3
Protein folding and degradation							
6	10 kDa heat shock protein, mitochondrial	*Acromyrmex echinatior*	gi|332019712	11.7/3.18	18.0/9.43	72	3/14
2	10 kDa heat shock protein, mitochondrial	*Acromyrmex echinatior*	gi|332019712	12.6/3.17	18.0/9.43	46	2/11
22	Peptidyl-prolylcis-transisomerase 5	*Harpegnathos saltator*	gi|307211461	24.7/3.73	22.4/8.77	67	1/4
60	FK506-binding protein 14	*Camponotus floridanus*	gi|307180846	28.3/8.39	14.3/4.57	144	4/38
67	Calreticulin	*Acromyrmex echinatior*	gi|332021110	68.5/8.50	45.3/4.46	79	3/6
76	Cyclophilin-like protein	*Nylanderia nr. pubens*	gi|292397870	16.3/5.03	18.0/8.89	48	4/17
83	Ubiquitin	*Harpegnathos saltator*	gi|307192162	9.1/5.61	7.7/5.76	198	3/55
91	Peptidyl-prolyl cis-trans isomerase 5	*Acromyrmex echinatior*	gi|332025731	20.2/5.02	22.0/8.85	80	2/12
106	Proteasome subunit alpha type-6	*Camponotus floridanus*	gi|307177334	30.8/5.38	27.7/7.56	40	2/6
(128)	26S protease regulatory subunit 8	*Harpegnathos saltator*	gi|307212064	51.8/5.02	45.8/8.55	139	5/17
243	Ubiquitin-conjugatingenzyme E2 variant 2	*Camponotus floridanus*	gi|307179132	16.3/6.19	16.4/6.59	104	3/27
245	Heat shock protein	*Trichogramma chilonis*	gi|284180155	13.4/6.01	8.8/6.51	141	2/20
282	Hypothetical protein SINV_11930 (Peptidyl-prolyl cis-trans isomerase)	*Solenopsis invicta*	gi|322798830	22.2/7.91	19.3/4.69	111	3/23
286	Heat shock protein beta-1	*Camponotus floridanus*	gi|307183305	30.9/6.66	29.5/6.37	326	5/25
287	Heat shock protein beta-1	*Camponotus floridanus*	gi|307183305	32.6/6.72	29.5/6.37	42	2/11
311	26S protease regulatory subunit 6A	*Camponotus floridanus*	gi|307190289	69.7/7.55	47.9/4.98	567	10/34
312	Hsc70-interacting protein	*Harpegnathos saltator*	gi|307215258	66.0/7.73	31.3/4.56	206	3/14
313	PREDICTED: heat shock 70 kDa protein cognate 3	*Apis florea*	gi|380030032	107/7.45	106/5.71	427	7/8
314	PREDICTED: heat shock 70 kDa protein cognate 3	*Megachile rotundata*	gi|383848513	109/7.49	106/5.52	311	5/7

							e coverge
(317)	26S protease regulatory subunit 6B	*Camponotus floridanus*	gi|307172856	71.3/7.35	45.8/5.16	48	1/2
318	26S protease regulatory subunit 6B	*Camponotus floridanus*	gi|307172856	74.1/7.28	45.8/5.16	263	5/16
319	Hypothetical protein SINV_14312 (60 kDa heat shock protein, mitocondrial)	*Solenopsis invicta*	gi|322787697	89.4/7.31	60.3/5.60	336	7/18
320	PREDICTED: 60 kDa heat shock protein, mitochondrial-like	*Apis mellifera*	gi|66547450	91.3/7.28	60.5/5.64	371	6/12
321	Hypothetical protein SINV_14312 (60 kDa heat shock protein, mitocondrial)	*Solenopsis invicta*	gi|322787697	90.0/7.20	60.3/5.60	305	6/16
322	Mitochondrial-processing peptidase subunit beta	*Harpegnathos saltator*	gi|307207091	67.2/7.16	53./5.77	355	6/11
338	Heat shock 70 kDa protein cognate 5	*Camponotus floridanus*	gi|307181923	104/6.86	72.3/6.37	547	8/12
(342)	Heat shock 70 kDa protein cognate 4	*Camponotus floridanus*	gi|307176326	106/6.97	71.7/5.43	541	9/21
347	Proteasome subunit alpha type-1	*Camponotus floridanus*	gi|307180286	42.0/6.57	31.1/5.91	196	4/15
363	Prefoldin subunit 3	*Camponotus floridanus*	gi|307172404	29.4/7.25	22.1/5.27	94	3/18
Cell signaling							
55	Calmodulin	*Camponotus floridanus*	gi|307181039	14.8/9.62	17.7/4.14	94	3/25
(100)	Hypothetical protein EAG_02089 (C-type lectin)	*Camponotus floridanus*	gi|307166128	28.9/5.69	27.0/6.30	84	1/6
226	Arginine kinase	*Harpegnathos saltator*	gi|307197996	48.5/6.48	40.0/5.75	276	5/23
Antioxidant activity							
78	Hypothetical protein SINV_03933 (Peroxiredoxin-5, mitocondrial)	*Solenopsis invicta*	gi|322796535	16.1/5.41	20.3/9.06	107	1/9
98	Mn superoxide dismutase	*Apis mellifera ligustica*	gi|33089106	23.0/5.37	24.7/9.11	121	2/12
229	PREDICTED: peroxiredoxin-6-like	*Bombus terrestris*	gi|340718481	29.6/6.32	25.4/5.46	56	1/6
247	Probable phospholipid hydroperoxide glutathione peroxidase	*Harpegnathos saltator*	gi|307192508	18.8/5.55	19.3/6.96	140	2/15
253	2-cys peroxiredoxin	*Bombus ignites*	gi|227976948	16.7/6.65	21.9/6.90	46	1/5
289	Hypothetical protein SINV_03768 (Peroxiredoxin-6)	*Solenopsis invicta*	gi|322797657	31.2/6.57	26.5/5.98	64	1/4
290	PREDICTED: peroxiredoxin-6-like	*Bombus terrestris*	gi|340718481	30.5/6.54	25.4/5.46	81	1/6
364	Phospholipid hydroperoxide glutathione peroxidase	*Acromyrmex echinatior*	gi|332027619	24.7/7.80	38.2/6.54	46	2/11
369	Peroxiredoxin 1	*Acromyrmex echinatior*	gi|332021321	28.9/5.06	21.8/5.94	116	1/7
Transport							
34	Similar to PREDICTED:	*Megachile*	gi|38385358	14.8/5.0	15.2/6.3	136	2/10

Spot No. [a]	Protein [b]	Organism	Accession number [c]	Exper. MW/pI [d]	Theor. MW/pI [e]	Mascot score [f]	Peptides matched /Sequence coverge
	myelin P2 protein-like	*rotundata*	0	3	7		
(75)	Fatty acid-binding protein, muscle	*Acromyrmex echinatior*	gi|332024570	14.4/5.06	15.6/6.43	52	2/16
(75)	Myelin P2 protein	*Harpegnathos saltator*	gi|307206040	14.4/5.06	19.8/6.64	138	5/16
105	Electron transfer flavoprotein subunit beta	*Acromyrmex echinatior*	gi|332025657	31.8/5.48	27.7/6.92	44	1/4
107	Electron transfer flavoprotein subunit beta	*Acromyrmex echinatior*	gi|332025657	32.0/5.35	27.7/6.92	86	2/10
183	Electron transfer flavoprotein subunit alpha	*Camponotus floridanus*	gi|307181675	37.0/5.11	35.7/8.97	50	1/3
249	Myelin P2 protein	*Harpegnathos saltator*	gi|307206040	14.8/6.66	19.7/6.64	145	3/9

Spot No. [a]	Protein [b]	Organism	Accession number [c]	Exper. MW/pI [d]	Theor. MW/pI [e]	Mascot score [f]	Peptides matched /Sequence coverge
Oxidation-reduction processes							
26	3-hydroxyacyl-CoA dehydrogenase type-2	*Acromyrmex echinatior*	gi|332024263	35.5/3.05	30.3/8.70	113	6/13
(96)	3-hydroxyacyl-CoA dehydrogenase type-2	*Acromyrmex echinatior*	gi|332024263	33.9/5.01	30.3/8.70	64	1/4
(128)	Hypothetical protein SINV_12515 (Hydroxysteroid dehydrogenase-like protein 2)	*Solenopsis invicta*	gi|322801306	51.8/5.02	42.9/8.83	95	1/4
130	Probable medium-chain specific acyl-CoA dehydrogenase, mitochondrial	*Harpegnathos saltator*	gi|307199032	54.5/5.15	42.5/8.15	106	1/3
201	Hypothetical protein SINV_02533 (Dihydrolipoyldehydrogenase)	*Solenopsis invicta*	gi|322790475	75.8/5.97	59.0/8.54	225	4/10
202	Hypothetical protein SINV_02533 (Dihydrolipoyldehydrogenase)	*Solenopsis invicta*	gi|322790475	75.1/5.95	59.0/8.54	73	2/7
315	Protein disulfide-isomerase	*Harpegnathos saltator*	gi|307207787	80.7/7.84	56.3/4.73	249	3/6
316	Protein disulfide-isomerase	*Harpegnathos saltator*	gi|307207787	79.7/7.86	56.3/4.73	193	4/6
333	Proteindisulfide-isomerase A6	*Camponotus floridanus*	gi|307167982	69.3/6.99	48.6/5.14	185	4/8
336	Protein disulfide-isomerase A3	*Acromyrmex echinatior*	gi|332023180	92.5/6.79	56.1/5.66	184	5/9
(344)	Short/branched chain specific acyl-CoA dehydrogenase, mitochondrial	*Camponotus floridanus*	gi|307182564	90.2/6.72	44.6/6.21	50	1/2
(348)	Retinal dehydrogenase 1	*Camponotus floridanus*	gi|307178537	48.6/6.77	53.5/5.46	64	1/2
349	Short/branched chain specific acyl-CoA dehydrogenase, mitochondrial	*Harpegnathos saltator*	gi|307202129	48.9/6.84	43.0/6.06	211	4/15
(350)	Retinal dehydrogenase 1	*Camponotus floridanus*	gi|307178537	51.3/6.88	53.5/5.46	48	2/3
351	Hemocyanin	*Acromyrmex*	gi|33202519	66.5/6.1	85.2/6.8	51	1/1

48

Spot No. [a]	Protein [b]	Organism	Accession number [c]	Exper. MW/pI [d]	Theor. MW/pI [e]	Mascot score [f]	Peptides matched /Sequence coverge
		echinatior	8	5	5		
Other processes							
23	Phosphatidylethanolamine-binding protein homolog	*Bombus impatiens*	gi|350403780	24.6/4.02	23.1/8.85	82	1/6
(27)	Cuticle protein 21	*Camponotus floridanus*	gi|307175910	34.5/4.78	26.1/6.20	59	2/9
(27)	PREDICTED: cuticle protein	*Nasonia vitripennis*	gi|156548084	34.5/4.78	35.0/7.29	32	1/3
(32)	Poly(A)-specific ribonuclease PARN	*Camponotus floridanus*	gi|307167442	54.9/3.29	65.5/6.35	41	1/1
(45)	Non-specific lipid-transfer protein	*Harpegnathos saltator*	gi|307194938	93.9/5.02	60.0/8.66	38	2/4
51	Flexible cuticle protein 12	*Acromyrmex echinatior*	gi|332023422	11.4/8.51	11.3/4.50	59	1/12
59	Myosin light chain alkali	*Harpegnathos saltator*	gi|307208335	16.9/8.57	17.3/4.57	152	4/37
65	Hypothetical protein SINV_02991 (Calumenin-B)	*Solenopsis invicta*	gi|322796781	51.4/8.51	40.0/4.55	79	3/10
70	PREDICTED: hexamerin-like	*Bombus terrestris*	gi|340721852	143/8.4	120/6.19	53	1/1
(96)	Voltage-dependent anion-selective channel	*Harpegnathos saltator*	gi|307198439	33.9/5.01	30.9/8.21	75	1/3
(99)	Cuticle protein 21	*Camponotus floridanus*	gi|307175910	28.7/5.77	26.1/6.20	42	1/3
152	Uncharacterized glycosyl transferase AER61	*Acromyrmex echinatior*	gi|332019577	55.3/5.77	45.8/8.51	32	1/3
153	PREDICTED: dehydrodolichyl diphosphate synthase-like	*Bombus impatiens*	gi|350413088	53.9/5.76	35.1/7.67	42	1/4
169	PREDICTED: dehydrodolichyl diphosphate synthase-like	*Bombus impatiens*	gi|350413088	48.0/6.05	35.1/7.67	32	1/4
170	PREDICTED: dehydrodolichyl diphosphate synthase-like	*Bombus impatiens*	gi|350413088	46.7/6.05	35.1/7.67	31	1/4
174	PREDICTED: dehydrodolichyl diphosphate synthase-like	*Bombus impatiens*	gi|350413088	45.0/5.97	35.1/7.67	33	1/4
230	Phosphatidylethanolamine-binding protein 1	*Acromyrmex echinatior*	gi|332028806	26.5/6.17	13.8/9.36	69	3/41
295	Ferritin subunit	*Acromyrmex echinatior*	gi|332027165	35.9/7.08	26.0/5.66	60	3/14
299	Nucleoplasmin-like protein	*Acromyrmex echinatior*	gi|332017234	29.9/7.91	24.2/4.67	49	1/4
302	Chondroitin proteoglycan-2	*Harpegnathos saltator*	gi|307212770	41.0/7.90	29.7/5.20	103	2/7
330	Hypothetical protein SINV_15827 (Regucalcin)	*Solenopsis invicta*	gi|322800197	47.5/7.06	42.7/5.35	50	1/3
334	Selenium-binding protein 1-A	*Acromyrmex echinatior*	gi|332021867	88.1/6.82	52.7/6.99	150	2/6
335	Selenium-binding protein 1-A	*Acromyrmex echinatior*	gi|332021867	89.4/6.92	52.7/6.99	161	3/9
337	Selenium-binding protein 1-A	*Camponotus floridanus*	gi|307191199	91.0/7.01	52.5/5.49	83	2/5

49

Spot No. [a]	Protein [b]	Organism	Accession number [c]	Exper. MW/pI [d]	Theor. MW/pI [e]	Mascot score [f]	Peptides matched /Sequence coverge
339	Transferrin	*Acromyrmex echinatior*	gi|332029256	120/6.82	79.4/5.47	185	4/6
340	Transferrin	*Solenopsis invicta*	gi|62912066	125/6.74	78.6/5.66	174	4/6
341	Transferrin	*Acromyrmex echinatior*	gi|332029256	123/6.89	79.4/5.47	172	4/5
(342)	Hypothetical protein SINV_08631 (Hexamerin)	*Solenopsis invicta*	gi|322781221	106/6.97	103/6.66	36	1/1
343	Transferrin	*Solenopsis invicta*	gi|62912066	124/6.96	78.6/5.66	139	3/5
(344)	Selenium-binding protein 1-A	*Acromyrmex echinatior*	gi|332021867	90.2/6.72	52.7/6.99	171	3/8
354	PREDICTED: hexamerin-like	*Bombus terrestris*	gi|340721852	45.2/6.20	120/6.19	36	1/0
355	PREDICTED: hexamerin-like	*Bombus terrestris*	gi|340721852	46.2/6.34	120/6.19	42	1/0
357	PREDICTED: hexamerin-like	*Bombus terrestris*	gi|340721852	46.5/6.23	120/6.19	44	1/0
359	PREDICTED: hexamerin-like	*Bombus terrestris*	gi|340721852	53.7/6.22	120/6.19	50	1/0
Unclassified function							
(24)	Muscle protein 20-like protein	*Solenopsis invicta*	gi|285027697	25.9/4.24	20.5/8.48	171	2/17
102	PREDICTED: protein lethal (2) essential for life-like	*Megachile rotundata*	gi|383852382	29.6/5.60	22.5/5.50	132	2/19
103	PREDICTED: protein lethal (2) essential for life-like	*Megachile rotundata*	gi|383852382	30.5/5.60	22.5/5.50	102	2/14
268	Hypothetical protein SINV_12721 (Natterin-3)	*Solenopsis invicta*	gi|322791066	16.2/7.65	15.7/4.86	66	1/7
Unknown function (no putative conserved domains were detected)							
21	Hypothetical protein EAI_12686	*Harpegnathos saltator*	gi|307195245	24.6/3.31	25.6/9.20	60	1/4
25	Hypothetical protein EAI_12686	*Harpegnathos saltator*	gi|307195245	29.0/3.11	25.6/9.20	56	2/8
31	Hypothetical protein SINV_13437	*Solenopsis invicta*	gi|322793390	49.1/3.18	40.8/9.04	107	1/4
(32)	Hypothetical protein EAG_16350	*Camponotus floridanus*	gi|307188535	54.9/3.29	43.7/9.07	98	4/9
(33)	Hypothetical protein SINV_13437	*Solenopsis invicta*	gi|322793390	47.6/3.89	40.8/9.04	66	2/8
35	Hypothetical protein SINV_13437	*Solenopsis invicta*	gi|322793390	55.1/4.67	40.8/9.04	116	2/6
(38)	Hypothetical protein SINV_13437	*Solenopsis invicta*	gi|322793390	48.9/4.21	40.8/9.04	104	1/4

Spot No. [a]	Protein [b]	Organism	Accession number [c]	Exper. MW/pI [d]	Theor. MW/pI [e]	Mascot score [f]	Peptides matched /Sequence coverge
(39)	Hypothetical protein SINV_13437	*Solenopsis invicta*	gi|322793390	48.7/4.08	40.8/9.04	113	1/4
43	PREDICTED: hypothetical protein LOC10068051	*Nasonia vitripennis*	gi|345487017	18.0/4.58	24.0/9.03	34	1/6
44	Hypothetical protein SINV_13437	*Solenopsis invicta*	gi|322793390	35.0/4.20	40.8/9.04	86	1/4
47	Hypothetical protein SINV_13437	*Solenopsis invicta*	gi|322793390	103/3.94	40.8/9.04	104	1/4
48	Hypothetical protein	*Solenopsis*	gi|322793390	102/4.29	40.8/9.0	101	1/4

	SINV_13437	*invicta*	0		4		
49	Hypothetical protein SINV_13437	*Solenopsis invicta*	gi|322793390	103/4.64	40.8/9.04	98	1/4
50	Hypothetical protein SINV_13437	*Solenopsis invicta*	gi|322793390	92.8/4.64	40.8/9.04	62	1/4
(99)	Hypothetical protein G5I_06293	*Acromyrmex echinatior*	gi|332025071	28.7/5.77	27.3/8.62	38	1/2
(125)	Hypothetical protein SINV_13437	*Solenopsis invicta*	gi|322793390	43.3/5.02	40.8/9.04	44	1/4
161	PREDICTED: hypothetical protein LOC100743670 isoform 1	*Bombus impatiens*	gi|350411203	52.1/5.96	42.6/8.95	32	1/3
180	hypothetical protein EAG_07856	*Camponotus floridanus*	gi|307189789	43.4/6.12	35.4/9.31	152	2/6
224	PREDICTED: hypothetical protein LOC100743670 isoform 1	*Bombus impatiens*	gi|350411203	76.2/6.57	42.6/8.95	31	1/3
275	Hypothetical protein SINV_01247	*Solenopsis invicta*	gi|322797002	18.3/7.46	22.0/5.79	95	3/23
280	Hypothetical protein EAG_04387	*Camponotus floridanus*	gi|307188291	18./7.92	17.3/5.02	80	1/8
293	Hypothetical protein SINV_03310	*Solenopsis invicta*	gi|322793661	33.9/6.37	30.3/6.01	140	2/10
368	Hypothetical protein SINV_13437	*Solenopsis invicta*	gi|322793390	49.8/5.01	40.8/9.04	48	1/4

[a] Spot numbers according to Figure 1, numbers in brackets when more than one protein was identified; [b] Protein names in brackets indicate the most likely protein obtained after BLASTP of the hypothetical protein sequences. [c] Accesion numbers in NCBInr protein database; [d] Experimental molecular weight and *pI*; [e] Theoretical molecular weight and *pI*; [f] Mascot score reported after searching against the *Hymenoptera* subset of the NCBInr protein database, scores ≥30 indicate identity or extensive homology ($p < 0.05$).